27 July 2009 Submitted to the TC4 Special Issue of JGR-Atmospheres

Convective and wave signatures in ozone profiles over the equatorial Americas: Views from TC4 (2007) and SHADOZ

Anne M. Thompson,[1] Alaina M. Luzik,[1,2] Gary A. Morris,[3] John E. Yorks,[1,4] Sonya K. Miller,[1] Brett F. Taubman,[5] Gé Verver,[6] Holger Vömel,[7] Melody A. Avery,[8] Johnathan W. Hair,[8] Glenn S. Diskin,[8] Edward V. Browell,[8] Jéssica Valverde Canossa,[9] Tom L. Kucsera,[10] Christopher A. Klich,[1] Dennis L. Hlavka[4]

[1] The Pennsylvania State University, Department of Meteorology, 503 Walker Building, University Park, PA 16802-5013 USA; anne@met.psu.edu; smiller@psu.edu; cok5018@psu.edu

[2] Now at National Weather Service Mid-Atlantic Flood Forecast Group, State College, PA 16803; alaina.luzik@noaa.gov

[3] Valparaiso University, Dept of Physics and Astronomy, Valparaiso, IN 46383 USA; gary.morris@valpo.edu

[4] SSAI of Lanham, MD 20706 USA; also at NASA/Goddard Space Flight Center, Greenbelt, MD 20771 USA; john.e.yorks@nasa.gov; dennis.l.hlavka@nasa.gov

[5] Appalachian State University, Dept of Chemistry, Boone, NC 28608; 828-262-7847; taubmanbf@appstate.edu

[6] KNMI (Royal Dutch Meteorological Institute), de Bilt, NL; ge.verver@knmi.nl

[7] DWD- Deutscher Wetterdienst, GRUAN - Lindenborg, Germany; Holger.voemel@dwd.de

[8] NASA/Langley Research Center, MS 401B, Hampton, VA 23681; melody.a.avery@nasa.gov; glenn.s.diskin@nasa.gov; johnathan.w.hair@nasa.gov; edward.v.browell@nasa.gov

[9] Laboratorio de Análisis Ambiental, Escuela de Ciencias Ambientales, Universidad Nacional P.O.Box: 86-3000 Heredia, Costa Rica; 00506-88694960; jvalverde25@gmail.com

[10] Univ Maryland Baltimore County - GEST, Baltimore, MD 21228; also at NASA/Goddard Space Flight Center, 301-614-6046; Tom.l.kucsera@nasa.gov

Keywords: Upper Troposphere/Lower Stratosphere; Ozonesondes; Tropical tropopause Layer; Gravity waves; Stratosphere-troposphere exchange

Running Head -

Thompson et. al.: TC4 and SHADOZ Costa Rica and Panamá Ozone and Waves

Thompson et. al.: TC4 and SHADOZ Costa Rica and Panamá Ozone and Waves

Convective and wave signatures in ozone profiles over the equatorial Americas: Views from TC4 (2007) and SHADOZ

Abstract. During the TC4 (Tropical Composition, Clouds and Climate Coupling) aircraft and ground campaign in July-August 2007, daily ozonesondes were launched over coastal Panamá, at Las Tablas (LTP, 8N, 80W), 300 km SW of Panamá City, and several times per week at Alajuela, Costa Rica (ACR, 10N, 84W). Wave activity, detected most prominently in 100-300 m thick O_3 laminae within the TTL (tropical tropopause layer), occurred in 40% (LTP) and 50% (ACR) of the soundings. These layers, associated with vertical displacements and classified as gravity waves ("GW," probably Kelvin waves) by the laminar identification method of *Grant et al.* [1998] and *Thompson et al.* [2007a], occur with similar structure and frequency over the Paramaribo (6N, 55W) and San Cristóbal (1S, 90W) SHADOZ (Southern Hemisphere Additional Ozonesondes) sites. GW-labeled laminae in individual LTP and ACR soundings correspond to cloud outflow (indicated by DC-8 tracers, TC4 satellite and aircraft imagery), confirming convective initiation of equatorial waves. Layers representing quasi-horizontal displacements, referred to as Rossby waves (RW) by the laminar technique, are robust features, particularly in soundings from 23 July to 5 August over LTP. The features associated with RW correspond to stratospheric influence, confirmed by relative dryness and/or reduced CO, and sometimes to transport of pollution. Comparison of LTP and ACR ozone budgets with 1999-2007 June-July-August (JJA) Paramaribo and San Cristóbal soundings shows that TC4 is typical of climatology for the equatorial Americas. Overall during TC4, convection and associated waves appear to dominate ozone transport in the TTL but intrusions from the extra-tropics persist throughout the free troposphere.

1. Introduction

Ozone in the tropical troposphere reflects an interaction of photochemical and dynamical factors. The marine atmosphere is usually unpolluted, largely because the boundary layer (BL) is a region of photochemical loss [*Piotrowicz et al.*, 1991]. This is a consequence of slow formation (low NO_x conditions; *McFarland et al.*, 1979; *Thompson et al.*, 1993) or, in exceptional cases, rapid loss from active halogens [*Read et al.*, 2008]. In the mid- and upper troposphere (UT) mixed sources converge [*Thompson et al.*, 1996]. Pollution near and far, stratospherically influenced air, and lightning add to O_3 formation, the latter at rates according to time since the lightning episode (*Thompson et al*, 1997; see *Cooper et al.* [2006] and *Bertram et al.* [2007] for analyses of lightning influence in mid-latitude convection). Ozone from the extra-tropics may enrich free tropospheric ozone as well [*Randel et al.,* 2007].

Examination of ozone profiles from sondes or aircraft over remote tropical sites reveals the free troposphere (FT) as a region of low O_3 (< 30 ppbv; *Thompson et al.*, 2003a) alternating with layers of elevated O_3 (sometimes > 100 ppbv; *Newell et al.,* 1999). From a climatology of O_3 and P-T-U soundings taken through SHADOZ [*Thompson et al.,* 2003a,b; *Loucks*, 2007], SOWER [Stratospheric Ozone and Water in Equatorial Regions; *Hasebe et al.,* 2007*; Takashima and Shiotani*, 2007] and related campaigns, the structure of the tropical UT and lower stratosphere (LS) has been deduced. Individual pollution layers in the FT are observed at Réunion, Fiji, Samoa, San Cristóbal, and Ascension [*Thompson et al.,* 2003b; *Oltmans et al.,* 2001; 2004; *Randriambelo et al.,* 2003]. Reduced O_3 layers often characterize the UT and TTL (tropical tropopause layer; *Fuglistaeler et al.,* 2009), typically from 8-14 km where convective outflow of low-O_3 BL air takes place. If O_3 in the UT and TTL averages to lower concentrations than in the mid-troposphere, an "S-shape" profile results [*Folkins et al.*, 2000], a distinct pattern over the western Pacific and eastern Indian Oceans.

The laminar identification (LID) method, based on the relationship of O_3 and potential temperature gradients (*Teitelbaum et al.,* 1994; *Pierce and Grant*, 1998; *Thompson et al.,* 2007a; 2008), interprets persistent O_3 layers in terms of two general wave-types. In the tropics, Rossby waves (RW) represent horizontal displacement; these tend to correlate with filaments of extra-tropical air or with pollution from long-range transport. When the SHADOZ dataset (> 3700 profiles) is analyzed with the LID technique, RW signatures are found to be present in < 20% of the soundings [*Loucks, 2007; Thompson et al.,* 2009]. However, in the TTL, signatures of convectively-generated gravity waves (GW) occur in 40-90% of the SHADOZ sondes, depending on location and season [*Thompson et al.,* 2009]. Near the tropopause, GW are usually identified with Kelvin waves. Transient Kelvin waves associated with O_3 have been observed in sondes [*Fujiwara et al.,* 1998; 2001] over the western and eastern Pacific.

Wave activity over the eastern Pacific and central America has received less attention. Robust GW and RW signals were noted during the Milagro/INTEX-B/IONS-06 (Intercontinental Transport Experiment; INTEX Ozonesonde Network Study) campaigns over Mexico City (19N, 99W) and Houston (30N, 95W) in March-May 2006, two locations [*Thompson et al.,* 2008] that are essentially sub-tropical when northern hemisphere spring flows link them to central America [*Fast et al.,* 2007].

The TC4 (Tropical Composition, Cloud, and Climate Coupling) mission in July-August 2007 offered an opportunity to characterize O_3 profiles closer to the equator than the IONS-06 soundings associated with INTEX-B/Milagro. TC4 [*Toon et al.*, 2009] investigated mechanisms of tropical convection, chemical transformation in convective systems and the impacts of deep convection on constituent transport, dehydration and cirrus formation. Aircraft sampling from San Jose, Costa Rica (10N, 84W), with three NASA platforms, the DC-8, WB-57 and ER-2, was well-suited for comparisons with ozonesonde-radiosonde profiles and with an instrumented ground site near the Panamá Bight. Most flights were south of the Intertropical Convergence Zone (ITCZ), which was located at 12-13N during the experiment [*Toon et al.,* 2009]. Regular SHADOZ [*Thompson et al.,* 2003a] sonde launches from Costa Rican (Alajuela, 10N, 84W, referred to here as ACR) were augmented during TC4 and daily soundings were made over Las Tablas, Panamá (LTP, 7.8N, 80W) from the NATIVE (Nittany Atmospheric Trailer and Integrated Validation Experiment) sampling system.

In this paper, we first describe mean properties of free tropospheric (FT) and LS O_3 over ACR and LTP during TC4 **(Section 2)**. Second, O_3 budgets based on LID and expressed as column amounts affected by GW and RW, provide a consistent framework for examining dynamic influences within the sonde profiles (**Section 3.1**). Third, case studies of sondes and ancillary aircraft, radar and satellite measurements are used to corroborate wave designations, with convection for GW or stratospheric influences or pollution for RW (**Section 3.2**). In **Section 3.3** context for the TC4 observations is given by June-July-August (JJA) Costa Rican sondes in 2006, and a 9-year record of sondes from SHADOZ launches [*Thompson et al.,* 2003a,b] at Paramaribo (5.8N, 55W) and San Cristóbal (1S, 90W). We address the following questions:

> How does FT O_3 over LTP and ACR in 2007 compare to JJA O_3 over Costa Rica in 2005 and 2006? How do LTP and ACR O_3 during TC4 compare to O_3 over the Paramaribo and San Cristóbal SHADOZ sites in 2007?

> How does 2007 JJA ozone at Paramaribo and San Cristóbal compare to other years for which soundings are available at these sites (1999 - 2006)?

2. **Experimental. Observations and Methods of Analysis**.

2.1 Ground & Aircraft

Continuous surface O_3 measurements at Las Tablas (8N, 80W) were made during the period 13 July to 8 August 2007 with a TECO Model 49 C ozone analyzer. Carbon monoxide (TECO Model 48CTL), NO and NO_y (TECO Model 42CY) and SO_2 (TECO Model 43C-TLE) were also measured, along with particle size distribution (SMPS, Scanning Mobility Particle Sizer). All measurements can be viewed at <http://ozone.met.psu.edu/NATIVE/TC4.html>. Calibrations of O_3, CO, and SO_2 were made prior to and directly after the campaign with instrument grade gases (Airgas, Inc.). Calibration of NO and NO_y was performed daily with instrument grade NO (Airgas, Inc.). Catalytic conversion efficiency was tested before and after the campaign and remained close to 100%.

2.2 Ozone Profiles and P-T-U Profiles

All ozone profile data analyzed here were taken with electrochemical concentration cell (ECC) instruments coupled with standard radiosondes, as described in *Thompson et al.* [2003; 2007a]. The locations of Las Tablas and the SHADOZ sites referred to here appear in **Table 1**. At Las Tablas, a 0.5% KI buffered solution was used with ENSCI ozonesondes, a combination that optimizes the O_3 measurement [*Smit et al.*, 2007; *Thompson et al.*, 2007b; *Deshler et al.,* 2008]. Vertical resolution is effectively 50-100 m [*Smit et al.*, 2007], sufficient to detect stable layers of locally elevated (or suppressed) O_3. Vaisala radiosondes, Model RS-80, were used to collect P-T-U (pressure-temperature-humidity) data. For nine of the 25 LTP sondes during TC4 the humidity data are unreliable above ~300-500 hPa due to suspected sensor icing. Ozone profiles from LTP are viewable at <http://ozone.met.psu.edu/Panama_Data/

index.html>. Although each ozonesonde is internally calibrated prior to launch, the LTP sondes were routinely compared to the TECO O_3 for 5-10 minutes prior to launch; agreement is within the stated precision of each technique (5%; see Figure 1 in *Morris et al.,* 2009).

Ozone over Alajuela was measured with ENSCI ECC sondes with 1% KI with reduced (0.1%) buffer; RS-80 radiosondes with a cryogenic frost-point hygrometer were used for P-T-U. At both sites, most launches took place in early afternoon local time to capture Aura [*Schoeberl et al.*, 2006], Aqua and CALIPSO satellite overpass [*Toon et al.,* 2009]. At Paramaribo, ozone is measured with SPC (Science Pump Corporation) ECC sensors, using 1% fully buffered sensing solutions in tandem with RS-80 radio-sondes to 2005 and RS-92 radiosondes thereafter [*Peters et al.,* 2003; *Fortuin et al.,* 2006]. Relative to total ozone from the TOMS (Total Ozone Mapping Spectrometer) and OMI (Ozone Monitoring Instrument) satellites, total O_3 from the sondes over Paramaribo is ~10% higher. This effect is greatest in the stratosphere (Figure 6 in *Thompson et al.*, 2007b) and has little impact on analyses of profiles below 20 km (~70 hPa). For San Cristóbal, SPC type ECC sondes are used with 1% KI/0.1% buffered solutions after 2006. Until then, 2% unbuffered KI sensing solutions were employed [*Johnson et al.,* 2002; *Thompson et al.,* 2007b] with Vaisala RS80 radiosondes. Total O_3 over San Cristóbal is ~7% lower than satellite total O_3 during the SHADOZ period [*Thompson et al.*, 2007b]. This typifies Pacific and Indian Ocean sites where tropospheric O_3 is lower than the algorithm used in TOMS (to 2005) and OMI (2005 onward) retrievals. Images and data for all Costa Rican (late 2005 start), Paramaribo (1999-present) and San Cristóbal (1999-present) ozonesonde and P-T-U profiles are available at <http://croc.gsfc.nasa. gov/shadoz> and at the World Ozone and Ultraviolet Data Centre, <http://woudc.org>.

Aircraft data used most often in analysis of the soundings are: O_3 from the FASTOZ *in-situ* instrument [*Avery et al*., 2009], uv-DIAL and CO on the DC-8; the Cloud Physics Lidar (CPL) and Cloud Radar System [*McGill et al.,* 2004; *Hlavka et al.,* 2009]. Regional cloud and convective information comes from meteorological analyses and GOES imagery, as archived by *Toon et al*. [2009].

2.3 Ancillary Data

As for IONS-04 and IONS-06 [*Thompson et al*., 2007a; *Thompson et al.,* 2008], tracers for O_3 origins include: (1) RH from the radiosonde PTU profiles; (2) Ertel's potential vorticity (pv; 1 pvu = 10^{-6} m^2s-1/K) computed from the Goddard Earth Observing System Assimilation Model (GEOS-version 4; *Bloom et al*., 2005); (3) forward and backward air-parcel trajectories for each launch location and date, calculated with the kinematic version of the GSFC trajectory model *[Schoeberl and Sparling,* 1995] using GEOS meteorological fields at a 1x1-degree grid. Lightning and lightning-exposure images are also used to describe potential O_3 influences, as are absorbing aerosol data from OMI, trajectory-enhanced aerosol-exposure images and OMI NO_2 amounts. All back-trajectories in the TC4 region, aerosol and lightning data and trajectory-mapped exposure products are at the GSFC TC4 website: <http://croc.gsfc. nasa.gov/tc4>.

The lightning data provided by NASA/MSFC are based on the CRLDN (Costa Rican Lightning Detection Network). The WWLLN (Worldwide Lightning Location Network) data [*Rodger et al.,* 2006] were obtained by NASA/GSFC during TC4. The CRLDN detection efficiencies for total lightning (cloud and ground flashes) decline with distance from Costa Rica and are estimated at ~40% over LTP based on comparison with TRMM/LIS (Tropical Rainfall Measuring Mission/Lightning Imaging Sounder) overpass data. The WWLLN has more even coverage but its detection efficiency for total flashes is estimated at 25% on average based on TRMM/LIS and CRLDN comparisons (see TC4 website; *Bucsela et al.,* 2009) but with considerable uncertainty. Because lightning data use here is qualitative, ie to link sources with O_3 laminae through trajectories, uncertainties in detection do not detract from our interpretations. In selected case studies, additional trajectories were run with the NOAA Hysplit model (*Draxler and Rolph*, 2003).

2.4 Analysis for Wave Influences

In the LID (Laminar Identification; *Thompson et al.,* 2007a; 2008) technique, O_3 and potential temperature (*θ)* laminae, as described in *Teitelbaum et al.* [1994; 1996] and *Pierce and Grant* [1998] are used to identify signatures of RW or GW; a schematic appears in **Figure 1**. Two analyses are performed with the LID results. First, for each sounding, the contributions of RW and GW above the boundary layer (BL) to the tropopause (for FT contributions) or to 20 km (for FT and LS, including the TTL) are computed by integrating the amount of O_3 within a given layer and adding up all the RW and GW segments. Dobson Units (DU) are used; one DU = 2.69×10^{16} cm^{-2}. The amount of O_3 within the FT or FT-TTL-LS column not identified with RW or GW is labeled "other" in the budgets. The BL top is determined by taking the most negative second derivative of θ between 0.4 and 2.5 km [*Yorks et al.*, 2009]. Mean BL heights are Panamá, 1.4 km; Costa Rica, 1.9 km (above a 0.95 km surface); Paramaribo, 1.4 km; San Cristóbal, 1.0 km. Second, for an ensemble of soundings, wave frequencies at a given altitude are calculated from the percentage of soundings within the sample set that have laminae with the RW or GW designation.

For determination of FT LID O_3 budgets **(Section 3)**, a chemical "ozonopause" is employed (white line, **Figure 2;** cf *Browell et al.,* 1996; *Stajner et al.*, 2008). *Thompson et al.* [2007a] showed that FT O_3 columns can differ significantly under certain conditions, depending on the use of O_3 or thermal tropopause. Such occurrences are infrequent in mid-latitudes (< 10% in IONS-04 or IONS-06 soundings; *Dougherty*, 2008) and are assumed negligible at the tropical sites studied here.

3. Results and Discussion: July-August 2007

3.1. Overview of Ozone Profiles over LTP and ACR

From curtains of ozone mixing ratio over Las Tablas and Alajuela **(Figure 2)** the following features emerge: (1) The BL is higher over ACR than LTP although approximately 10% more O_3 is found in the LTP BL than ACR due to pollution from Panamá City and occasionally from South American biomass burning. (2) The TTL extends lower over LTP than over ACR; at LTP the TTL is lowest on 26-28 July.

There appear to be more episodes of high convection (blue shade, 12-14 km) over ACR than LTP; the latter may be biased by more samples. Consequently, there is lower O_3 in the ACR mean O_3 profile between 11-14 km **(Figure 3a)** than LTP **(Figure 3b)**, giving a more distinct "S" shape to the ACR O_3 profile, similar to profiles over Pacific SHADOZ sites (*Folkins et al.,* 2000; 2006; cf *Kley et al.,* [1996] and UT O_3 minima in TC4 discussed by *Petropavloskikh et al.* [2009]). The O_3 maximum is at 8-9 km over LTP and ACR. Ozone soundings during IONS-06 (<http://croc.gsfc.nasa.gov/intexb/ions06>) August 2006 sampling over Mexico City (19N, 99W), during the North American monsoon, also detected the highest UT O_3 at 8-9 km with an O_3 minimum at 12-14 km (*Thompson et al.,* 2008; Fig 5). Note that during DC-8 spirals in TC4, FASTOZ [*Avery et al.,* 2009] ozone profiles showed the characteristic S-shape. At the 8-11 km region, where O_3 was suppressed, owing to clean BL origins, the CO was sometimes enhanced [*Avery et al.,* 2009], denoting convective transport from below.

Compared to ACR (**Figure 2a)**, mid-tropospheric ozone (4-12 km) is higher over LTP **(Figure 2b)**, signified by more greens and golds below 6 km, especially during the period from 24-29 July 2007. This includes the period of lowest LTP tropopause (see **Section 3.2.2** for the correspondence of the elevated FT O_3 to stratospheric influence and discussion of surface O_3 and CO at that time).

Figure 4a shows that the O_3 labeled GW is concentrated in the TTL and LS over both LTP and ACR and the corresponding frequencies are similar to those at the Paramaribo and San Cristóbal SHADOZ sites (**Figure 4b).** The latter depicts wave frequencies averaged for 1999-2007, which are nearly identical to June-July-August statistics. The wave structure in **Figures 4a,b** compares well to other SHADOZ tropical (*Loucks*, 2007; *Thompson et al.,* 2009) and NH subtropical locations (Figure 4 in *Thompson et al.*, 2008). It was inferred from LTP and ACR O_3 curtains (**Figure 2**) and mean profiles (**Figure 3**) that convective activity may be higher during TC4 over ACR than LTP. Assuming that GW frequency scales with convection, this would account for higher GW frequency in the TTL and LS over ACR than LTP (**Figure 4a**).

For Panamá, laminae amplitude is 10-20% (not shown), with values > 15% occurring below 3 km. Where GW is 15% at 2 km, the process represented may be convective mixing near the top of the BL. At a second GW frequency maximum over ACR, 6 km, convective cloud outflow may be taking place. FT O_3 associated with GW over LTP and ACR is approximately 15% of the FT column (**Table 2**). For LTP, RW occurs as frequently in the FT below 10 km as in the TTL and LS (**Figure 4a**; cf **Figure 1**). In about half the days with soundings at both ACR and LTP, LTP O_3 in the 3-6 km region is 40-50 ppbv in contrast to ~30 ppbv over ACR (cf **Figure 3** mean O_3 profiles).

In **Figure 5a**, where data from days with dual LTP and ACR launches are illustrated, O_3 budgets through the FT, TTL and LS to 20 km as determined from the LID method [*Thompson et al.,* 2008; *Yorks et al.,* 2009] show ACR to have less O_3. The mean O_3 column to 20 km is 42 DU over LTP (tropospheric O_3 budgets for all LTP and ACR soundings appear in **Figures 5b,c)**, with the FT O_3 column averaging ~28

DU (**Table 2**). The tropospheric O_3 column (~19 DU, on average) fractions of ozone to 20 km are similar for ACR and LTP.

3.2 Case Studies with Convective and Wave Influence

Days with coincident launches at LTP and ACR (**Figure 5a; Table 3**) offer an opportunity to compare ozone profiles at the two sites and to use TC4 aircraft data, satellite imagery and meteorological products to interpret convective and wave influences. All of the dates listed in **Table 3** display convective signatures as denoted by a substantial amount of ozone affected by GW, typically > 10 DU of the O_3 column in the FT and stratosphere to 20 km. In some cases convection appears to influence principally the TTL and in other cases the lower or middle FT (cf **Figure 1**).

The TC4 period started with active convection over the Costa Rica-Panama region and the adjacent Pacific. This is corroborated by satellite and aircraft imagery in flights through 22 July 2007 [*Toon et al.,* 2009]. From 23 July through 2 August, mean integrated O_3 segments designated GW declined in most soundings (**Figure 5b**), as the GW-affected region retreated from the upper FT to above 17 km. During this time the amount of column O_3 affected by RW increased compared to the pre-24 July period. More convective conditions returned after 2 August 2007, when targeted sampling by the ER-2, DC-8 and WB-57 took place [*Toon et al.,* 2009]. In **Section 3.2.1** we examine profiles on days for which GW denotes high convective activity at ACR and/or LTP. Verification of convective influence within O_3 and RH profile segments are typically made with tracer measurements from nearby aircraft sampling or with aircraft or satellite cloud imagery. Selected soundings with relatively high RW and low GW are examined **(Section 3.2.2)** to verify stratospheric influence or advection of pollution.

3.2.1 Cases with Elevated GW (Convectively-Generated)

Figure 6 depicts sonde temperature, RH and ozone for the LTP and ACR pairs on July days in which one or both sites display convective signature within the FT segment of the profiles (13, 19, and 22 July) and there was aircraft sampling (**Table 3)**.

13 July. Convective activity at LTP and ACR, as given by GW amount to 20 km, is similar (**Figure 5a)**. The fraction of FT ozone influenced by GW is similar in both cases (~20%; **Figures 5b,c)**. Over ACR the O_3 concentration averages ~40 ppbv from the surface to the tropopause, which is ~14-15 km (**Figure 6a**). The tropopause is also ~14 km over LTP, where the BL O_3 (20 ppbv) is less than over ACR. Ozone in the UT over LTP was greater than 50 ppbv. The RH profiles have considerable structure over both sites, with moister air over LTP than ACR. Evidence for convection over ACR comes from the DC-8 flight from California to San Jose, Costa Rica, on 13 July 2007. The last 100-150 km of the flight encompassed a descent near ACR at ~2100 UT time, after the aircraft had crossed the ITCZ. The DC-8 uv-DIAL image of O_3 (**Figure 7a)** captures the morphology of convective impact throughout the FT and TTL. North of the ITCZ (northern edge at 13N), the FT was penetrated by pollution O_3 (>80 ppbv) and aerosols traced to biomass fires interacting with convection. South of the ITCZ, just before descent, FT O_3 dropped to 40-50 ppbv, except for a localized O_3 minimum (< 30 ppbv) around 10 km (**Figure 7a),** similar to FT O_3 structure over ACR (**Figure 6a)**, and to the DC-8 FASTOZ O_3 during descent. The uv-DIAL aerosols (not shown) indicate a "clean" FT south of the ITCZ except for a thin cirrus layer at the tropopause, consistent with the soundings. Convective indicators, elevated methyl-hydrogen peroxide, lightning NO, ultrafine particles and CO (not shown; see flight report at <http://espo.nasa.gov/ tc4/docs>), penetrated south of the ITCZ. Inter-hemispheric transport from convective outflow is well known over the Atlantic [*Jonquières et al.,* 1998; *Thompson et al.*, 2000; *Edwards et al.*, 2003].

19 July. LTP and ACR budgets contrasted on this date, with more intense convective activity implied by the high GW fraction over LTP (**Figure 5a**). Even though the O_3 profiles do not look very different (**Figure 6b**), interpreting the subtle differences between the two sets of profiles illustrates both the capabilities and limitations of the LID. For example, there is no O_3 with a GW signature over ACR, implying little convection. This was verified by the 19 July ER-2 flight that sampled convective activity W-SW of ACR but found no cells nearby nor upwind (refer to <http://cpl.gsfc.nasa.gov> and to Figure 9 in *Toon et al.* [2009] for flight tracks and to *Hlavka et al.* [2009] for cloud and convective cell imagery from the CPL and Cloud Radar System [CRS). More than half of ACR FT O_3 is categorized as RW (**Figure 5c).** The corresponding segment, from ~4-11 km, is labeled in **Figure 6b.** If the RW designation implies advection of dehydrated filaments, that process could give rise to the thin low-RH laminae at 6, 7, and 8 km. For LTP, only from 10-15 km does the RW designation apply. This is consistent with a locally dry, high-O_3 layer (to 90 ppbv) from ~9-11 km in **Figure 6b**. However, at ~12-12.5 km, ie within the 10-15 km RW segment over LTP, O_3 is a minimum (drops to 70 ppbv) and RH increases. This thin layer corresponds to cloud outflow as indicated by GOES imagery (**Figure 7b)**; the cloud-top temperature in the image corresponds to ~12 km. Over LTP, convection leads to GW throughout the TTL, above 15 km. Thus, ~40% of the FT and LS O_3 to 20 km, 18 DU, is designated GW. Only 3-4 DU of GW O_3 is in the FT. **Figure 7b** shows that clouds do not appear over ACR. Contrast in convective properties is also implied by OMI NO_2 (**Figure 7c)** where a signal appears over LTP but not ACR, suggesting lightning (that produces NO that is in equilibrium with NO_2) is near LTP.

22 July. This is another day in which there is more O_3 identified as GW, perhaps implying more convection, over LTP than ACR (**Figure 5a-c)**. As for 19 July, most of the GW O_3 is concentrated in the TTL (very little FT GW O_3 is indicated in

Figure 7c). The ozone column amount over ACR on 22 July is lower than on 19 July because mid-FT O_3 averages 20 ppbv less (cf **Figures 6b,c)**. The convective contrast between ACR and LTP is confirmed by satellite imagery (see ER-2 flight report for 22 July 07 at <http://espo.nasa.gov/tc4/docs>). GOES at 1600 UTC, during the ACR sounding, displays no convection near ACR. The ER-2 sampled near LTP on 22 July, where cloud and precipitation CPL-CRS imagery (**Figure 7c)** depicts streaming cirrus at 12.5-13 km with ~13.5-14 km cloud top. The LID wave structure for the LTP sounding suggests GW above 14 km, right above a localized O_3 minimum (black profile, **Figure 6c)**, consistent with cloud structure observed by the ER-2 (**Figure 7c).**

<u>3 August.</u> The 20-km O_3 budgets over ACR and LTP represent a slight contrast (**Figure 5a)** but the magnitude of the FT GW and RW segments are nearly the same (**Figures 5b,c).** The soundings themselves (**Figure 8a**) suggest a contrast in convective influence. Over ACR, O_3 mixing ratios above 6 km increased steadily, averaging > 80 ppbv in the 6-13 km segment (**Figure 8a),** even though there is a GW segment over ACR at 9-12 km. Above 8 km, the RH drops off sharply, suggesting stratospheric air. A mostly RW segment corresponds to 13-17 km, bracketing the ozonopause, which is 2 km lower over ACR than over LTP (**Figure 2)**.

Over LTP the GW segment that was confined above 17 km on 2 August, returns as a robust signal in the UT and TTL (**Figure 8a)** from 13-20 km (see **Section 3.3.2)**. The DC-8 and ER-2 sampled not far from LTP (**Figure 9a**) near active convection (refer to GOES image with flight tracks for all three aircraft on 3 August; Figure 16 in *Toon et al.,* [2009]). Convective influence is pronounced over LTP and ACR. The upper of two O_3 minima, at 10-15 km (**Figures 8a and 9b**, with DC-8 spiral measurements), corresponds to cloud outflow recorded by satellite imagery. **Figure 9c,** the CPL-CRS product, indicates persistent cirrus at 13-15 km, confirming outflow coincident with the broad O_3 minimum in **Figure 8a**. A second O_3 minimum with elevated CO at 5km **(Figure 9b)** is located where there is evidence of cloud aerosol in CPL-CRS imagery (**Figure 9c**).

4 - 5 August. From 3 August to 4 August there was a sharp transition in the profiles over ACR and LTP **(Figures 8a,b)** that is reflected in the O_3 budgets **(Figures 5a-c)**. The relatively dry layer at 8-12 km over LTP becomes moister and the high-$O_{3,}$ ~ 80 ppbv, declines to 50 ppbv. A sharp ozonopause (16 km) characterizes both ACR and LTP profiles. The GW O_3 budgets to 20 km are identical over ACR and LTP on 4 August. The "S-shape" over LTP, in which a thick O_3 minimum was centered at 13 km on 4 August, is replaced by a nearly uniform 40 ppbv on 5 August **(Figures 8a,b)** such that FT O_3 over LTP drops from 33 DU to 22 DU, the lowest ozone column in the TC4 period **(Figure 5b).** There is also a decline in FT O_3 over ACR **(Figure 5c).** The upper FT through TTL and LS is characterized by a very robust GW (above 11 km over ACR, 12 km over LTP). However, given the reduced O_3 concentrations in this region, the FT GW budgets (3 DU over ACR, 5 DU over LTP) are fairly low. Although RH profiles are relatively moist from 4-10 km over ACR and LTP on 4 August, the corresponding laminae (**Figure 8b)** retain the RW classification of the prior day. In the FT, RW O_3 is 3 DU over ACR and 5 DU over LTP. On 5 August, over LTP, aircraft sampling confirms FT stratospheric origins (below) below the segment designated RW.

From 4 August to 5 August transitions continue in vertical O_3 structures over ACR and LTP (**Figure 8c).** The GW signal, that began at 11 km extending through the TTL on 4 August over ACR (12 km over LTP) retreated to 15 km (14 km over LTP) on 5 August. As a consequence, FT O_3 over LTP associated with GW declined from 5 DU to 3 DU. The sharp ozonopause dropped ~1 km from 4 August to 5 August, although the UT O_3 structure looks unchanged. Segments designated RW on 5 August were slightly displaced from the prior day but remained prominent between 6 and 12 km. Within this segment, O_3 concentrations over ACR were diminished. Between 7 and 12 km the mean was 75 ppbv on 3 August, 55 ppbv on 4 August and 45 ppbv on 5 August, with similar RH on the latter two days.

Over LTP, from 8 -12 km on 5 August, coinciding with an RW segment (**Figure 1** gives details of the laminar analysis), there is a several-km thick layer that is 20 ppbv above background (within the blue segment in **Figure 1**; see also **Figure 8c)**. The LTP sonde oscillated five times between 2.5 km and 5.1 km on the south end of a dissipating cell. The profile in **Figure 8c** and LID analysis are based on an average of the data between 2.5 and 5.1-km so the GW component may be under-estimated. During the two hours between the first and last ascent in the oscillation layer, O_3 concentrations increased by 4-12 ppbv. Analysis of this case by *Morris et al.* [2009] concludes that lightning NO production is responsible for much of the increase.

On 5 August, the DC-8 sampled over the Panama Bight, then spiraled SE of LTP (5.5 N 78W) over the Pacific in a cloudy area, detecting elevated O_3 (50-70 ppbv) and suppressed CO in a dry layer at 8-10 km, confirming stratospheric origins. The DC-8 noted cleaner than usual conditions at 11 km from updrafts of marine boundary layer air (**Figure 8c)**, although the DC-8 spiral and NATIVE sampling noted elevated pollutant concentrations near the surface due to biomass fires (see Flight notes at <http://www.espo.nasa.gov/tc4/docs>). ER-2 sampling aimed for convective cells just SW of LTP (~1540 and 1610 UTC) in Figure 19 in *Toon et al.,* 2009). On route back to Costa Rica, convection over the Pacific was detected (**Figure 9d).**

3.2.2 Cases with Elevated RW. Stratospheric and/or Advected Pollution

During the period 23 July through 28 July most sonde launches were at LTP. It was noted above that wave signals in the soundings from 23 to 31 July denoted less GW activity (less convection) and larger RW O_3 segments, implying more stratospheric influence. Evidence for stratospheric influence was observed in surface ozone and CO at NATIVE (**Figure 10**). On 23 July a normal diurnal O_3 cycle was observed (cf Figure 2 in *Morris et al.,* 2009), with a near-zero nocturnal minimum. However, on 24 July the O_3 minimum is closer to 15 ppbv, which causes the daily mean O_3 to increase from 17 ppbv on 23 July to 25 ppbv on 24 July. At this time, CO dropped below 90 ppbv, one of the lowest values during TC4, suggestive of stratospheric air (**Figure 10**). This was accompanied by a lower tropospheric wind shift from easterly to westerly. By 26 July, normal values for CO and O_3 were re-established. The LID analysis for 23 July at LTP was not valid, a condition that indicates active transition and no stable layers. However, two days illustrate important RW signals.

31 July. In **Figure 11a** the ozone and RH vertical structure from the soundings over ACR and LTP are remarkably similar except for a local O_3 minimum that is relatively moist over ACR at 12-14 km. Integrated GW and RW O_3 amounts at the two sites to 20 km (**Figure 5a**) are nearly identical. GW ozone occurs only in the LS (no GW segments in **Figures 5b,c**) implying an absence of convective influence, although below 6 km, RH averages 70-80% over both sites. During ER-2 sampling on 31 July SE of Costa Rica (Figure 16 in *Toon et al.,* 2009), CPL-CRS indicated cloud tops at 15-16 km but there were no cells or upwind convective influence over ACR.

Two FT local O_3 maxima in the ACR sounding at 7.5 and 8.5 km appear 0.5-1 km higher over LTP (**Figure 11a)**. The higher-altitude peak coincides with an RH minimum, suggesting a stratospheric contribution. Note that a distinct RW segment occurs at 4-8 km over ACR and half of the FT O_3 column (~ 10 DU) is classified as RW **(Figure 5c**). RW segments over LTP, although not continuous, occur between 7 and 15 km, giving a 10-DU FT O_3 column associated with RW, similar to ACR (**Figure 5b).**

2 August. ACR displays convective influence in terms of GW only from 11-15 km (**Figure 11c)**. An RW segment from 5-10 km appears to be explained by a dry stratospherically influenced layer from 4-9 km. The latter feature persisted to 3 August

(**Figure 8a)**; there were no 2 August flights. There is no GW signal at all over LTP on this day. However, there is RW signal from 2 to 17 km except for one unclassified segment, at 8-10 km. This extended feature is not as dry as over ACR but the RH over LTP decreases above 7 km. As for ACR the RW influence is retained over LTP even as convection picks up and is sampled on 3 August (**Figures 8a and 9a,b)**.

Of contrasts between the ozone over LTP and ACR, perhaps the most significant is in the mixed layer where the LTP mixing ratio averages ~35 ppbv and ACR drops below 20 ppbv. Trajectory analysis (not shown) near the surface give a possible indication for the contrast. Air parcel origins over ACR are marine but at LTP, near surface parcels passed over the Panama City region (not shown).

3.3 Wave Activity in Panamá and CR Profiles

Further context for interpreting convective influence over LTP and ACR is provided by wave frequencies for JJA over Paramaribo and San Cristóbal (**Figure 4b**), SHADOZ sites operating since 1999 [*Thompson et al.,* 2003a,b]. The amplitudes of individual layers and wave structure at the two latter sites resemble those for LTP and ACR (as in **Figure 1**). The GW frequencies at LTP and ACR resemble those at San Cristóbal and Paramaribo **(Figures 4a,b)**. Similar GW structure appears over equatorial Indian Ocean sites, eg Watukosek, Kuala Lumpur, that display the highest annually averaged GWF, ~60% [*Thompson et al.,* 2009]. The higher GWF at San Cristóbal is reflected in the GW fraction of JJA 2007 tropospheric ozone budgets. Although the tropospheric O_3 column averaged 25 DU, compared to 28 DU for LTP, the GW-affected O_3 is 25% for San Cristóbal compared to 15% for LTP **(Table 2)**. **Figure 4c**, that summarizes GW frequency on a monthly averaged basis over Paramaribo, shows that JJA has about half the maximum GWF, a typical December occurrence. The TC4 campaign was timed for the buildup of the northern sub-tropical convective season and the onset of the North American monsoon.

An interannual perspective on ozone budgets and convective influence appears in **Figure 12**, where mean JJA tropospheric column ozone (with segments for RW and GW) is displayed for CR (2006 only), Paramaribo and San Cristóbal from 1999-2007. Note that BL ozone is not included here; this amounts to 2 DU for San Cristóbal, 3.5 DU at Paramaribo and CR. At San Cristóbal, 2006 is a low-O_3 year compared to the six others, possibly due to a moderate El Niño [*Logan et al.*, 2008]. In the eastern Pacific, El Niño tends to enhance convective activity, mixing lower O_3 air from the BL throughout the troposphere. The GW-affected tropospheric ozone amount in 2006 is only slightly lower than normal San Cristóbal but the total tropospheric column dropped from a mean 22-23 DU (1999-2005; **Figure 12)** to 18 DU so the fraction is magnified. At ACR, 2006 tropospheric ozone is lower than 2007 (**Figure 12).**

General meteorological conditions of Paramaribo (6N), Panamá (8N), and Alajuela (10N) are similar, with the ITCZ migrating over each, but the three sites represent a gradient away from the equator. From the SHADOZ analyses of *Loucks* [2007] and *Thompson et al.* [2009], GW frequency diminishes away from the equator. A GWI (Gravity Wave Index) and Rossby Wave Index (RWI; **Figure 13**), based on the fraction of the O_3 column (in altitude segment to 20 km) that is encompassed by each designation provides a quantitative approach to comparing sonde-to-sonde and interannual variability. The GWI is larger (RWI smaller) at San Cristóbal than at Paramaribo, until more sporadic sampling at San Cristóbal after 2004 appears to compromise the statistics. The latter precludes conclusive linkage of GWI and RWI to climatic signals associated with an El Niño.

4. Summary

During TC4, in July and early August 2007, ozonesondes and radiosondes were launched several times/week at Alajuela, Costa Rica (10N, 84W) to characterize convective influences and TTL structure. At Las Tablas, Panamá (8N, 80W), a remote coastal site 300 km southwest of Panamá City, O_3 profiles from daily sondes, surface O_3, CO and other tracers were analyzed using meteorological fields and satellite observations. Laminar identification (LID), a technique that provides a systematic approach to classifying wave signatures in sounding data, gives a statistical perspective on the TC4 period as well as comparison to the longer-term SHADOZ sounding record at Paramaribo and San Cristóbal. The findings are summarized:

- GW influences, possibly due to semi-permanent Kelvin waves in the TTL and LS (cf *Grant et al.,* 1998; *Thompson et al.,* 2009) appeared in 40% of LTP sondes and 50% for ACR; the latter is similar to the JJA GW frequency in the TTL and LS over the San Cristóbal and Paramaribo SHADOZ sites.
- On average there is 35-40% more tropospheric column O_3 at LTP than ACR during TC4 and 20% more at LTP than at San Cristóbal, a remote marine station, 1400 km southwest of LTP.
- June-July-August soundings at Paramaribo and San Cristóbal suggest that 2007 was a "typical" year in terms of tropical equatorial O_3 amount and convective activity expressed in GW frequency. During 1999-2006, Paramaribo and San Cristóbal display a range of O_3 column amounts and convective influence that bracket the TC4 ACR and LTP values.

Classification of wave types through LID is validated through case studies in which aircraft and satellite observations support interpretation of convective influences (with the GW designation) and stratospheric signatures, corresponding to RW. Laminae of low-O_3 surface air injected into the FT through convection are detected by LID, frequently interleaved with stratospheric layers; subtle day-to-day variations are also captured. The pattern of convection inferred from LID over the course of TC4 is consistent with the meteorological evolution of the campaign [*Toon et al.,* 2009]. The early part of TC4, from 13-22 July 2007, was characterized by persistent GW throughout the TTL and segments of the FT. These signals diminished from 23 July until approximately 2 August, retreating to above the TTL, and replaced by RW segments in the lower and mid FT in many cases. The latter corresponds to strato-spheric influence or occasional pollution. After 2 August, GW activity resumed in the FT as convection strengthened and aircraft sampling intensified in the TC4 region.

Satellite and aircraft data along with sondes established the convection-GW linkage and demonstrated that stratospheric laminae interleaved with layers from convective outflow is a prevalent pattern in the equatorial Americas. In terms of TC4 objectives, our analysis of ozone structure strengthens the case for convection as a dominant mechanism for water vapor transport and cirrus formation in the TTL. The persistence of O_3 laminae of stratospheric origins throughout the free troposphere requires further investigation to determine the extent to which these layers are remnants of extra-tropical filaments or associated with localized equatorial waves.

Acknowledgments. We are grateful to NASA's Upper Air Research Program and Aura Validation (M. J. Kurylo; K. W. Jucks) that sponsored the Las Tablas and Alajuela TC4 soundings and ground-based measurements at Las Tablas. These programs, with NOAA support, also sponsor SHADOZ at Costa Rica and San Cristóbal. The Paramaribo station is sponsored by KNMI and the Suriname Meteorological Department. Additional analysis support came from NASA's Tropospheric Chemistry Program (J. H. Crawford, J. A Al-Saadi). Las Tablas measurements with the NATIVE trailer were assisted by A. Pino and L. Jordan (University of Panamá); A. M. Bryan and D. Lutz (Valparaiso Univ); J. L. Tharp (PSU). Costa Rican launches were made by UNA students K. Cerna, V. H. Beita, D. Gonzalez. Thanks to Mission Scientists M. R. Schoeberl and P. A. Newman for flight notes and to K. E. Pickering for discussing lightning data. NASA/MSFC supplied CRLDN data and NASA/GSFC provided WWLLN flashes. Thanks to EAB, BvdW, AOG (PSU) for analysis.

Table 1. Stations for which data are used. Further technical details given in Table A-1 in *Thompson et al.* (2003a) and in *Thompson et al.* (2007b).

Station	Latitude	Longitude	Co-Investigator/Sponsor
Las Tablas	7.8N	-80.	G. A. Morris, A. M. Thompson
San Cristóbal	-0.92	89.60	H. Vömel. INAMHI (National Inst. of Hydrology and Meteorology of Ecuador), M. V. A. Reyes
Paramaribo	5.81	-55.21	G. Verver & Met. Service Surinam
Heredia/Alajuela,	10.0	-84.1	H. Vömel; J. Valverde Canossa

Table 2. Free tropospheric ozone columns during June-July-August 2007. ACR mean omits 28 July sounding.

Station	GW O_3	RW	Other	Total
ACR - DU	2.9	8.2	9.3	20.4 DU
ACR - %	14	40	46	100
LTP - DU	3.94	13.2	10.8	28 DU
LTP - %	15	47	38	100
San Cris.- DU	5.5	7.5	12	25
San Cris.- %	24	28	48	100

Table 3. Summary of days with both Las Tablas (LTP) and Alajuela (ACR) sondes and corresponding TC4 flights.

Date	Flight	Date	Flight
13 July	DC-8	2 Aug.	---
19 July	ER-2	3 Aug.	DC-8, ER-2, WB-57
22 July	DC-8,ER-2	4 Aug.	---
28 July	--	5 Aug.	DC-8, ER-2, WB-57
31 July	DC-8, ER-2		

References

Avery, M. A., et al. (2009), Tropospheric ozone distribution by convection in the central American ITCZ region: Evidence from observations of ozone and clouds during the Tropical Composition, Cloud and Climate Coupling Experiment, *J. Geophys. Res.*, this issue.

Bertram, T., et al. (2007), Direct measurements of the convective recycling of the upper troposphere, *Science*, **315,** 816–820, doi:10.1126/science.1134548.

Bloom, S., et al. (2005), Documentation and validation of the Goddard Earth Observing System (GEOS) data assimilation system - Version 4. Technical Report Series on Global Modeling and Data Assimilation 104606.

Browell, E. V., et al. (1996), Ozone and aerosol distributions and air mass characteristics over the South Atlantic Basin during the burning season, *J. Geophys. Res.*, **101**, 24,043-24,068.

Bucsela, E., et al. (2009), Lightning-generated NOx seen by OMI during NASA's TC4 experiment, *J. Geophys. Res.*, this issue.

Cooper, O. R., et al. (2006), Large upper tropospheric ozone enhancements above mid-latitude North America during summer: In situ evidence from the IONS and MOZAIC ozone networks, *J. Geophys. Res.*, **111,** D24S05, doi: 10.1029/2006JD007306.

Deshler, T., et al. (2008), Balloon experiment to test ECC-ozonesondes from different manufacturers, and with different cathode solution strengths: Results of the BESOS flight, *J. Geophys. Res.*, **113,**D04307, doi:10.1029/2007JD008975.

Dougherty, K. M. (2008), The effect of ozonopause placement on tropospheric ozone budgets: An analysis of ozonesonde profiles from selected IONS-06 sites, MS Thesis, The Pennsylvania State University.

Draxler, R. R., and G. D. Rolph (2003), HYSPLIT (Hybrid Single-Particle Lagrangian Integrated Trajectory) model, http://www.arl.noaa.gov/ready/hysplit4.html, NOAA Air Resour. Lab., Silver Spring, MD.

Edwards, D. P., et al. (2003), Tropospheric ozone over the tropical Atlantic: A satellite perspective, *J. Geophys. Res.*, **108**, 4237, doi: 10.1029/2002JD002927.

Fast, J. D., et al. (2007), A meteorological overview of the MILAGRO field campaign, *Atmos. Chem. Phys.* **7,** 2233-2257.

Folkins, I., S. J. Oltmans, and A. M. Thompson (2000), Tropical convective outflow and near-surface equivalent potential temperatures, *Geophys. Res. Lett.*, **27**, 2549-2552.

Folkins, I., P. Bernath, C. Boone, K. Walker, A. M. Thompson, and J. C. Witte (2006), The seasonal cycles of O3, CO and convective outflow at the tropical tropopause, *Geophys. Res. Lett.*, **33,** L16802, doi:10.1029/2006GL026602.

Fortuin, P., et al. (2007), Origin and transport of tropical cirrus clouds observed over Paramaribo, Suriname (5.8°N, 55.2°W), *J. Geophys. Res.*, **112,** D09107, doi:10.1029/2005JD006420.

Fueglistaler, S., A. E. Dessler, T. J. Dunkerton, I. Folkins, Q. Fu, and P. W. Mote (2009), Tropical tropopause layer, *Rev. Geophys.*, **47,** RG1004, doi:10.1029/2008RG000267.

Fujiwara, M., K. Kita, and T. Ogawa (1998), Stratosphere-troposphere exchange of ozone associated with the equatorial Kelvin wave as observed with ozonesondes and rawinsondes, *J. Geophys. Res.,* **103**, No. D15, 19,173-19,182.

Fujiwara, M., F. Hasebe, M. Shiotani, N. Nishi, H. Vömel, and S. J. Oltmans (2001), Water vapor control at the tropopause by equatorial Kelvin waves observed over the Galápagos, *J. Geophys. Res.,* **28,** 3143-3146.

Fujiwara, M., et al. (2003), Ozonesonde observations in the Indonesian maritime continent: A case study on ozone rich layer in the equatorial upper troposphere, *Atmos. Env.*, **37**, 353-362.

Grant, W. B., R. B. Pierce, S. J. Oltmans, and E. V. Browell (1998), Seasonal evolution of total and gravity wave induced laminae in ozonesonde data in the tropics and subtropics, *Geophys. Res. Lett.* **25**, 1863-1866.

Hasebe, F., M. Fujiwara, N. Nishi, M. Shiotani, H. Vömel, S. Oltmans, H. Takashima, S. Saraspriya, N. Komala, and Y. Inai (2007), In situ observations of dehydrated air parcels advected horizontally in the Tropical Tropopause Layer of the western Pacific, *Atmos. Chem. Phys.*, 7, 803-813.

Hlavka, D., L. Tian, W. Hart, L. Li, M. McGill, and G. Heymsfield (2009), Vertical cloud climatology during TC4 derived from high-altitude aircraft merged lidar and radar, *J. Geophys. Res.*, this issue.

Johnson, B. J., S. J. Oltmans, H. Vömel, T. Deshler, C. Kroger, and H. G. J. Smit (2002), ECC ozonesondes pump efficiency measurements and sensitivity tests of buffered and unbuffered sensor solutions, *J. Geophys. Res.*, *107*(D19), 4393, doi: 10.1029/2001JD000557.

Jonquières, I., A. Marenco, A. Maalej, and F. Rohrer (1998), Study of ozone formation and transatlantic transport from biomass burning emissions over West Africa during the airborne Tropospheric Ozone Campaigns TROPOZ I and TROPOZ II, *J. Geophys. Res.*, **103**, 19,059–19,073.

Kley, D., Crutzen, P. J., H. G. J. Smit, H. Vömel, S. J. Oltmans, H. Grassl, and V. Ramanathan (1996), Observations of near-zero ozone levels over the convective Pacific: Effects on air chemistry, *Science*, **274**, 230–233.

Logan, J. A., I. Megretskaia, R. Nassar, L.T. Murray, L. Zhang, K.W. Bowman, H.M. Worden, and M. Luo (2008), Effects of the 2006 El Niño on tropospheric composition as revealed by data from the TES, *Geophys. Res. Lett.,* **35**, L03816, doi:10.1029/2007GL031698.

Loucks, A. L. (2007), Evaluation of dynamical sources of ozone laminae in the tropical troposphere and tropical tropopause layer, M.S. Thesis, Penn State University.

McFarland, M., D. Kley, J. W. Drummond, A. L. Schmeltekopf and R.M. Winkler (1979), Nitric oxide measurements in the equatorial Pacific region, *Geophys. Res. Lett.,* **6,** 605-609.

McGill, M. J., L. Li, W. D. Hart, G. M. Heymsfield, D. L. Hlavka, P. E. Racette, L. Tian, M. A. Vaughan, and D. M. Winker (2004), Combined lidar-radar remote sensing: Initial results from CRYSTAL-FACE, *J. Geophys. Res.*, **109**, D07203, doi:10.1029/2003JD004030.

Morris, G. A., et al. (2009), Observations of ozone production in a dissipating convective cell during TC4, *J. Geophys. Res.*, this issue.

Newell, R. N., V. Thouret, J. Y. N. Cho, P. Stoller, A. Marenco, H. G. Smit (1999), Ubiquity of quasi-horizontal layers in the troposphere, *Nature,* **398,** 316-319.

Oltmans, S.J., et al. (2001), Ozone in the Pacific tropical troposphere from ozonesonde observations, *J. Geophys. Res.*, **106**, 32503-32526.

Oltmans, S. J., et al. (2004), Tropospheric ozone over the North Pacific from ozonesonde observations, *J. Geophys. Res.*, **109,** D15S01, doi: 10.1029/2003JD003466.

Peters. W., P. Fortuin, H. Kelder, C.R. Becker, J. Lelieveld, P.J. Crutzen, and A.M. Thompson (2004), Tropospheric ozone over a tropical Atlantic station in the Northern Hemisphere: Paramaribo, Surinam (6°N, 55°W), *Tellus,* **56,** 21-34.

Petropavloskikh, I., et al. (2009), Low ozone bubbles observed in the tropical tropopause layer during the TC4 campaign in 2007, *J. Geophys. Res.*, this issue.

Pierce, R. B., and W.B. Grant (1998), Seasonal evolution of Rossby and gravity wave induced laminae in ozonesonde data obtained from Wallops Island, Virginia, *Geophys. Res. Lett.*, **25**, 1859-1862.

Piotrowicz, S. R., H. Bezdek, G. Harvey, and M. Springer-Young (1991), On the ozone minimum over the equatorial Pacific Ocean. *J. Geophys. Res.* **96,** 18679-18687.

Randel, W. J., D. J. Seidel, L. L. Pan (2007), Observational characteristics of double tropopauses, *J. Geophys. Res.*, **112,** D07309, doi:10.1029/2006JD007904.

Randriambelo, T., J-L. Baray, S. Baldy, A. M. Thompson, S. J. Oltmans, and P. Keckhut (2003), Investigation of the short-term variability of tropical tropospheric ozone, *Annales Geophysiques,* **21,** 2095-2106.

Read, K. A. et al. (2008), Extensive halogen-mediated ozone destruction over the tropical Atlantic Ocean, *Nature*, **453,** 1232-1235, doi: 10.1038/nature07035.

Rodger, C. J., S. Werner, J. B. Brundell, E. H. Lay, N. R. Thomson, R. H. Holzworth, and R. L. Dowden (2006), Detection efficiency of the VLF World-Wide Lightning Location Network (WWLLN): initial case study, *Ann. Geophys.*, 24, 3197-3214.

Schoeberl, M. R., and L.C. Sparling (1995), Trajectory modeling: Diagnostic tools in atmospheric physics, S. I. F. Course CXVI, edited by G. Fiocco and C. Visconti, North-Holland, Amsterdam.

Schoeberl, M. R., et al. (2006), Overview of the EOS aura mission, IEEE Trans., **44** (5), 1066-1074, doi:10.1109/TGRS.2005.861950.

Smit, H. G. J., et al. (2007), Assessment of the performance of ECC-ozonesondes under quasi-flight conditions in the environmental simulation chamber: Insights from the Jülich Ozone Sonde Intercomparison Experiment (JOSIE), *J. Geophys. Res.*, **112**, D19306, doi: 10.1029/2006JD007308.

Stajner, I., et al. (2008), Assimilated ozone from EOS-Aura: Evaluation of the tropopause region and tropospheric columns, *J. Geophys. Res.*, **113**, D15S32, doi:10.1029/2007JD008863.

Takashima, H., and M. Shiotani (2007), Ozone variation in the tropical tropopause layer as seen from ozonesonde data, *J. Geophys. Res.*, **112**, D11123, doi:10.1029/2006JD008322.

Teitelbaum, H., J. Ovarlez, H. Kelder, and F. Lott (1994), Some observations of gravity-wave-induced structure in ozone and water vapour during EASOE, *Geophys. Res. Lett.*, **21**, 1483-1486.

Teitelbaum, H., et al. (1996), The role of atmospheric waves in the laminated structure of ozone profiles a thigh latitude. *Tellus,* **48A,** 442–455.

Thompson, A. M., et al. (1993), SAGA-3 ozone observations and a photochemical model analysis of the marine boundary layer during SAGA-3, *J. Geophys. Res.*, **98**, 16955-16968.

Thompson, A. M., et al. (1996), Where did tropospheric ozone over southern Africa and the tropical Atlantic come from in October 1992? Insights from TOMS, GTE/TRACE-A and SAFARI-92, *J. Geophys. Res.*, **101**, 24,251-24,278.

Thompson, A. M., W.-K. Tao, K. E. Pickering, J. R. Scala, and J. Simpson (1997), Tropical deep convection and ozone formation, *Bull. Amer. Met. Soc.*, **78**, 1,043-1,054.

Thompson, A. M., B. G. Doddridge, J. C. Witte, R. D. Hudson, W. T. Luke, J. E. Johnson, B. J. Johnson, S. J. Oltmans, and R. Weller (2000), A tropical Atlantic paradox: Shipboard and satellite views of a tropospheric ozone maximum and wave-one in January-February 1999, *Geophys. Res. Lett.*, **27,**3317-3320.

Thompson, A. M., et al. (2003a), Southern Hemisphere Additional Ozonesondes (SHADOZ) 1998-2000 tropical ozone climatology. 1. Comparison with TOMS and ground-based measurements, *J. Geophys. Res.*, **108,** 8238, doi: 10.1029/2001JD000967.

Thompson, A. M., et al. (2003b), Southern Hemisphere Additional Ozonesondes (SHADOZ) 1998-2000 tropical ozone climatology. 2. Tropospheric variability and the zonal wave-one, *J. Geophys. Res.,* **108**, 8241, doi: 10.1029/2002JD002241.

Thompson, A. M., et al. (2007a), IONS (INTEX Ozonesonde Network Study, 2004). 1. Summertime UT/LS (Upper Troposphere/Lower Stratosphere) ozone over northeastern North America, *J. Geophys. Res.,* **112**, D12S12, doi: 10.1029/2006JD007441.

Thompson, A. M., J. C. Witte, H. G. J. Smit, S. J. Oltmans, B. J. Johnson, V. W. J. H. Kirchhoff, and F. J. Schmidlin (2007b), Southern Hemisphere Additional Ozonesondes (SHADOZ) 1998-2004 tropical ozone climatology. 3. Instrumentation, station variability, evaluation with simulated flight profiles, *J. Geophys. Res.*, **112,** D03304, doi: 10.1029/ 2005JD007042.

Thompson, A. M., J. E. Yorks, S. K. Miller, J. C. Witte, K. M. Dougherty, G. A. Morris, D. Baumgardner, L. Ladino, and B. Rappenglueck (2008), Tropospheric ozone sources and wave activity over Mexico City and Houston during Milagro/Intercontinental Transport Experiment (INTEX-B) Ozonesonde Network Study, 2006 (IONS-06), *Atmos. Chem. Phys.,* **8**, 5113-5125.

Thompson, A. M., A. L. Loucks, S. Lee, S. K. Miller (2009), Gravity and Rossby wave influences in the tropical troposphere and lower stratosphere based on SHADOZ (Southern Hemisphere Additional Ozonesondes) soundings, 1998-2007, *J. Geophys. Res.*, to be submitted.

Toon, O. B., et al. (2009), Planning and implementation of the Tropical Composition, Cloud and Climate Coupling Experiment (TC4), *J. Geophys. Res.*, this issue.

Yorks, J. E., A. M. Thompson, E. Joseph, and S. K. Miller (2009), The variability of free tropospheric ozone over Beltsville, Maryland (39N, 77W) in the summers 2004-2007, *Atmos. Environ.,* **43,** 1827-1838.

FIGURE CAPTIONS

Fig 1 Application of laminar identification (LID) method to typical sounding from Panamá. Segments within FT (free-troposphere), TTL (tropical tropopause layer), LS (lower stratosphere) are depicted along with normalized O_3 (solid line), potential temperature (dotted line) and correlation between the two quantities (dashed). Correlation criteria for Rossby waves (RW) are within vertical lines between -0.3 and +0.3 (light blue). The latter designation is used in discussion of profiles and budgets. For computation of the RW Index, a more restrictive criterion is used, namely, the corresponding O_3 layer amplitude must exceed 0.1 (10%), as in the darker blue. Gravity wave (GW) criterion of *Pierce and Grant* (1998; see their Figure 1) and *Thompson et al.* (2007a; Figure 3) calls for normalized O_3 and è correlation to reach 0.7 (vertical line; light green for budgets). For computation of the GW Index, only ozone within dark green is counted, i.e., the 10% layer-amplitude requirement is applied to O_3.

Fig 2 Curtain plots of ozone mixing ratio to 18 km during TC4 over (a) Alajuela, Costa Rica (ACR); (b) Las Tablas, Panamá (LTP). White line refers to the tropopause.

Fig 3 Mean profiles of ozone, temperature, relative humidity (RH) from surface to 20 km for: (a) Alajuela, Costa Rica (ACR); eight O_3 profiles with slight interference from volcanic SO_2 have been smoothed at 3 km. (b) Las Tablas, Panamá. In the latter case, seven questionable RH profile segments are omitted from mean.

Fig 4 (a) Frequency of GW occurrence over LTP, ACR during July-August 2007 TC4 sampling; (b) mean GW frequency over Paramaribo and San Cristóbal, based on all 1999-2007 profiles. Paramaribo did not launch during TC4; (c) annual cycle in GW frequency at Paramaribo. The latter is typical of tropical SHADOZ sites.

Fig 5 (a) Amounts of FT-TTL-LS O_3 (in DU) from top of the BL to 20 km, affected by GW, RW determined by LID [*Thompson et al.*, 2007a] based on O_3 and P-T-U soundings from days with both Las Tablas (LTP) and Alajuela (ACR) launches during TC4. (b) Same as (a) except for free tropospheric (FT) O_3 segment of all LTP soundings during TC4; (c) same as (b) for FT ozone over ACR.

Fig 6 Ozone, RH, temperature profiles at ACR and LTP for three days with convective influence at one or both sites, as denoted by GW-affected ozone. (a) 13 July 2007; (b) 19 July; (c) 22 July. Vertical bars refer to RW (blue) and GW (green) as described in Figure 1.

Fig 7 (a) Uv-DIAL image of ozone from DC-8 flight from California to Costa Rica. Ozone < 40 ppbv, purple, is near surface and also at cloud outflow level, ~ 10 km, south of the ITCZ; the latter is the cloudy region at 1945 UTC; (b) GOES image with cloud top temperature for 19 July 2007; cloud top location over LTP corresponds to GW-lamina, signifying convection, which is absent over ACR. (c) OMI NO_2 is higher over LTP than ACR; (d) convective cells on 22 July 2007 near LTP from ER-2 Cloud Physics Lidar and Cloud Radar System composite image [*Hlavka et al.*, 2009].

Fig 8 Profiles from days with active convection in August 2007 TC4 sampling (a) 3 August 2007; (b) 4 August; (c) 5 August. Labels as in Figure 6. For 5 August, the DC-8 O_3 measurement from profiling near LTP displayed a high-O_3 low-CO layer [*Avery et al.,* 2009] similar to the high-O_3, lower RH feature at 8-10 km in (c). Stratospheric origins are thus confirmed within profiles that reflect active convection. On 5 August, the ozonesonde package, caught in a dissipating convective cell, oscillated in updrafts and downdrafts (presumably due to icing) while undergoing photochemical ozone formation associated with lightning [*Morris et al.*, 2009]. Profiles corresponding to the oscillatory segment in (c) have been averaged so the GW pattern may not be captured below 7 km.

Fig 9 (a) 3 Aug 2007 flight track of DC-8 (red, with spiral over LTP, starred) and ER-2 (blue) superimposed on GOES-R cloud imagery enhanced with cloud-top height. Arrow indicates location of DC-8 spiral that resulted in (b) where ozone and CO indicate stratospheric influence from 6-8 km and convection at 5 km and above 8 km. ER-2 sampling produced (c) composite CPL-CRS image with convective cells at 7.5N, 80.5W. (d) same as (c) except for 5 August ER-2 sampling.

Fig 10 Evidence for RW signifying stratospheric impact at surface, from daily mean mixing ratios of (a) ozone; (b) CO measured from NATIVE in Las Tablas, Panamá (7.8N, 80N).

Fig 11 Profile sets of ozone and RH with more prominent RW influence and less GW ozone signature in FT. (a) 31 July 2007; (b) 2 August 2007.

Fig 12 Averaged ozone amounts (in DU) in FT affected by GW, RW determined by the laminar method using all soundings of O_3 and P-T-U from 1999-2007 for San Cristóbal, Paramaribo, and, since 2005, for Costa Rica. The 2007 designation at LTP is for the TC4 period. In 2007, SHADOZ Costa Rican sonde launches moved from Heredia to Alajuela, ~20 km distant.

Fig 13 Gravity and Rossby wave Indices (GWI, RWI) based on O_3 and P-T-U soundings from the SHADOZ sites: (a) Paramaribo, Suriname (6N, 55E); (b) San Cristóbal, Galapagos (1S, 90W).

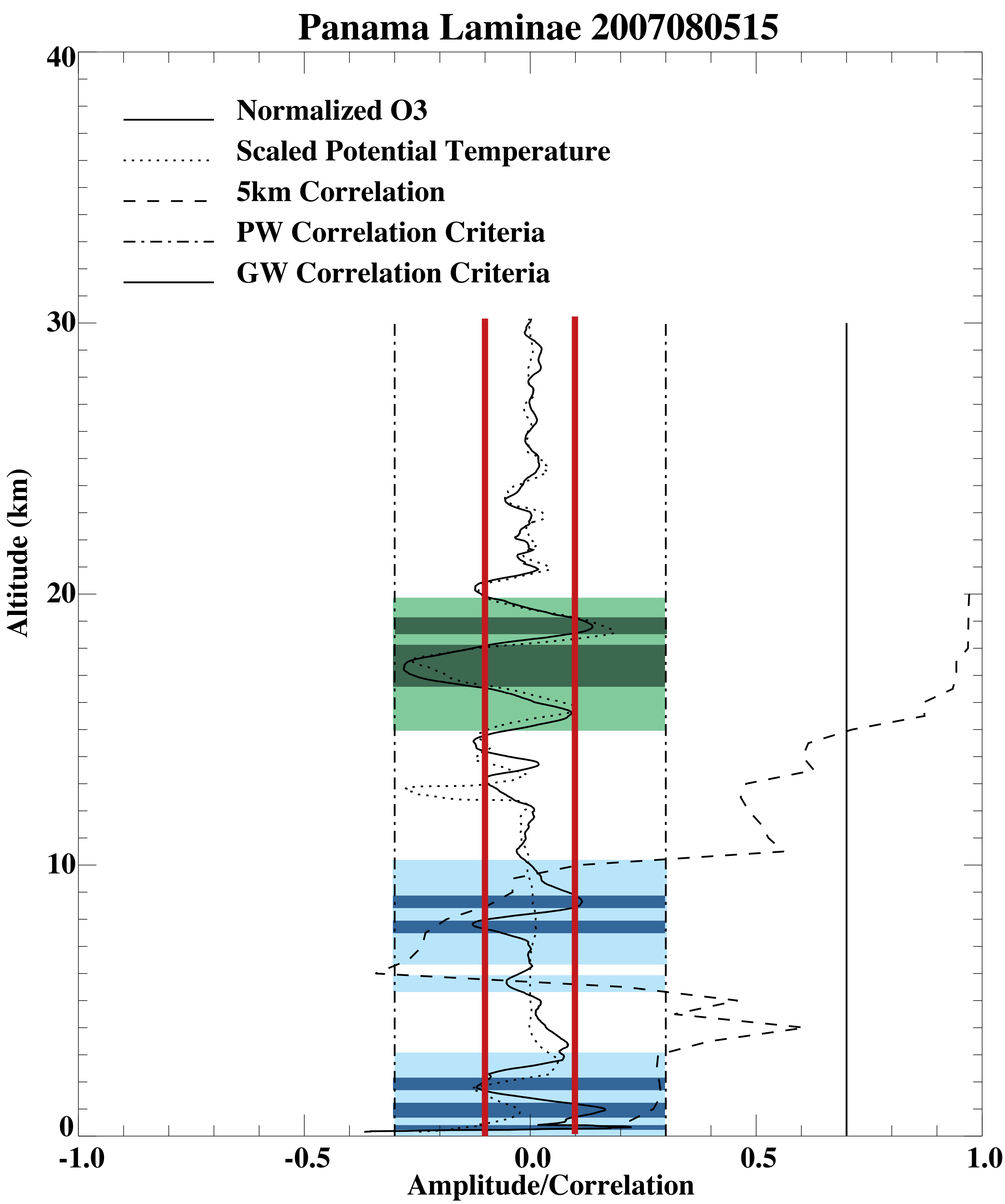

Panama Laminae 2007080515
Normalized O3
Scaled Potential Temperature
5km Correlation
PW Correlation Criteria
GW Correlation Criteria
Altitude (km)
0
10
20
30
40
-1.0
-0.5
0.0
0.5
1.0
Amplitude/Correlation

FIGURE 1

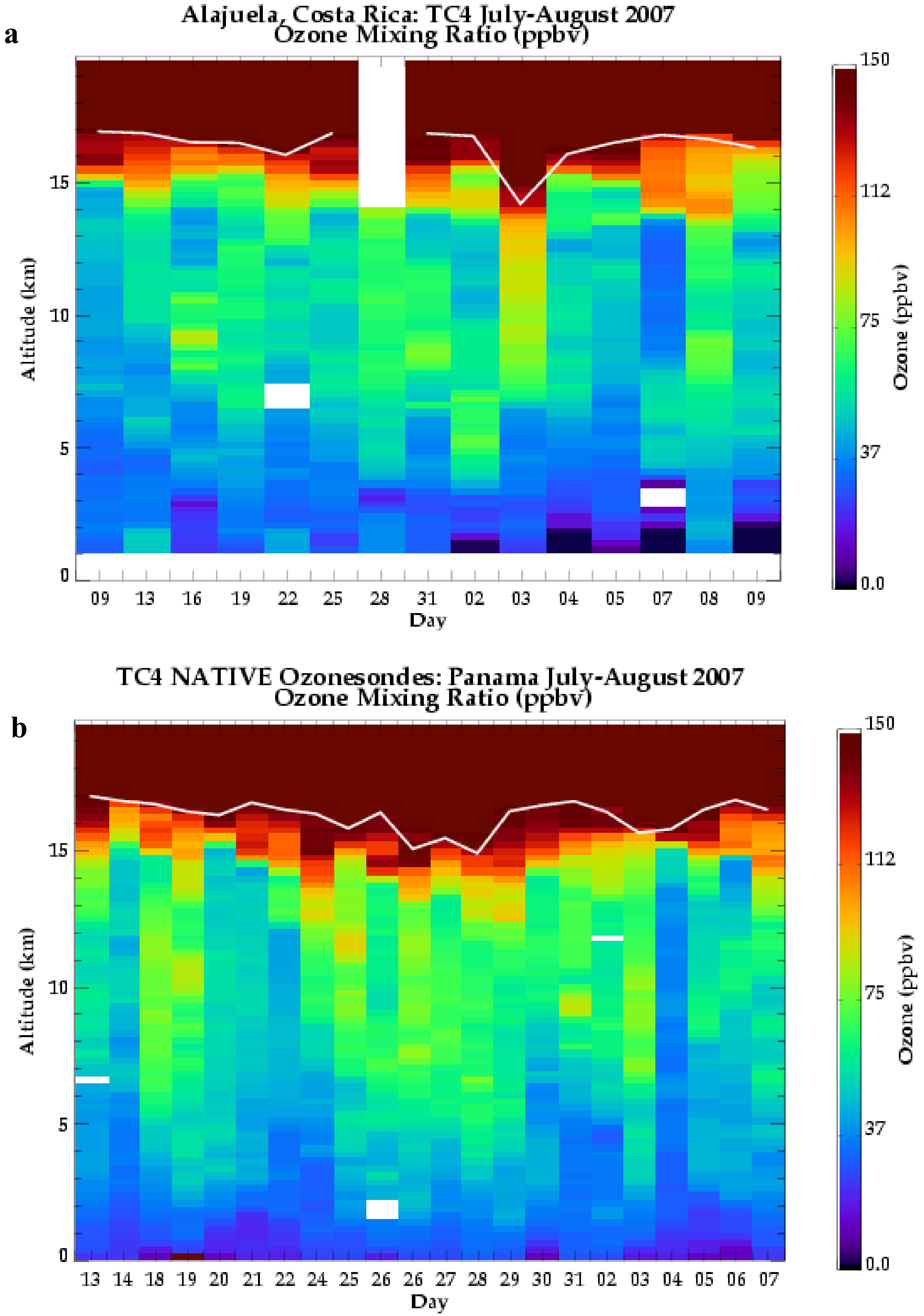
a
Alajuela, Costa Rica: TC4 July-August 2007
Ozone Mixing Ratio (ppbv)
Altitude (km)
0
5
10
15
09 13 16 19 22 25 28 31 02 03 04 05 07 08 09
Day
150
112
75
37
0.0
Ozone (ppbv)
b
TC4 NATIVE Ozonesondes: Panama July-August 2007
Ozone Mixing Ratio (ppbv)
Altitude (km)
0
5
10
15
13 14 18 19 20 21 22 24 25 26 26 27 28 29 30 31 02 03 04 05 06 07
Day
150
112
75
37
0.0
Ozone (ppbv)

FIGURE 2

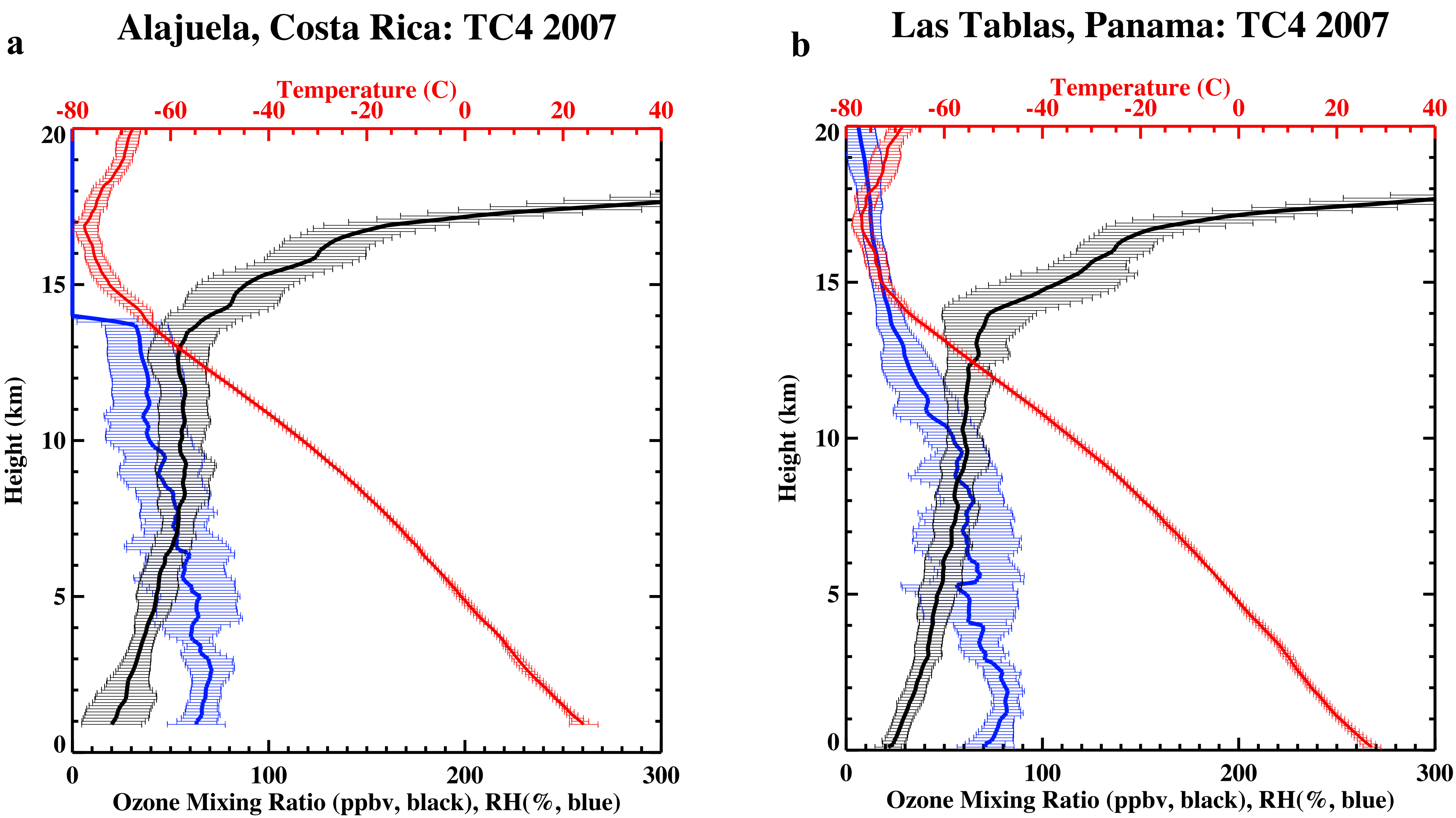
a
Alajuela, Costa Rica: TC4 2007
Temperature (C)
-80 -60 -40 -20 0 20 40
20
15
10
5
0
Height (km)
0 100 200 300
Ozone Mixing Ratio (ppbv, black), RH(%, blue)
b
Las Tablas, Panama: TC4 2007
Temperature (C)
-80 -60 -40 -20 0 20 40
20
15
10
5
0
Height (km)
0 100 200 300
Ozone Mixing Ratio (ppbv, black), RH(%, blue)

FIGURE 3

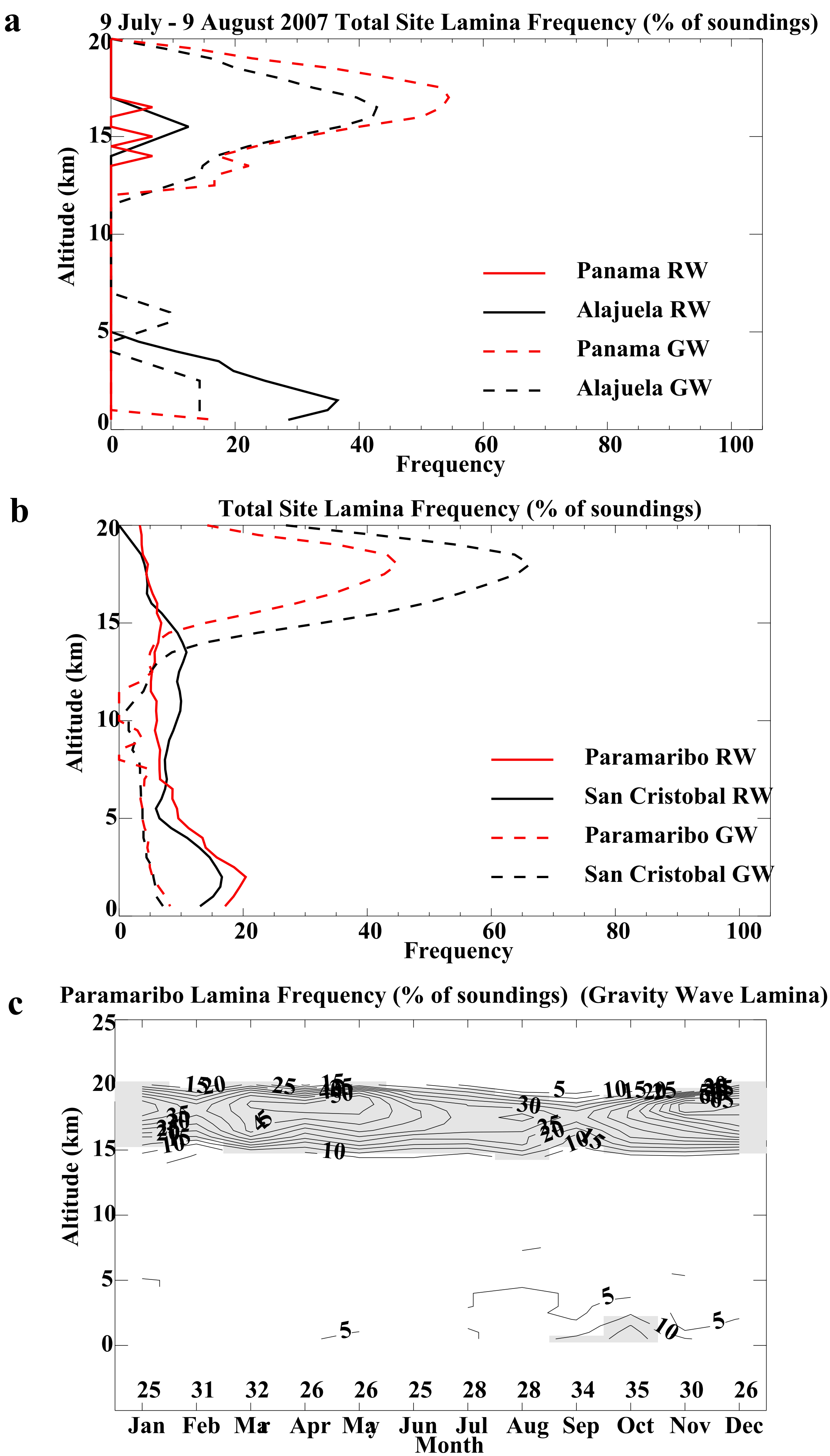
a
9 July - 9 August 2007 Total Site Lamina Frequency (% of soundings)
Altitude (km)
Frequency
Panama RW
Alajuela RW
Panama GW
Alajuela GW
b
Total Site Lamina Frequency (% of soundings)
Altitude (km)
Frequency
Paramaribo RW
San Cristobal RW
Paramaribo GW
San Cristobal GW
c
Paramaribo Lamina Frequency (% of soundings) (Gravity Wave Lamina)
Altitude (km)
25 31 32 26 26 25 28 28 34 35 30 26
Jan Feb Mar Apr May Jun Jul Aug Sep Oct Nov Dec
Month

FIGURE 4

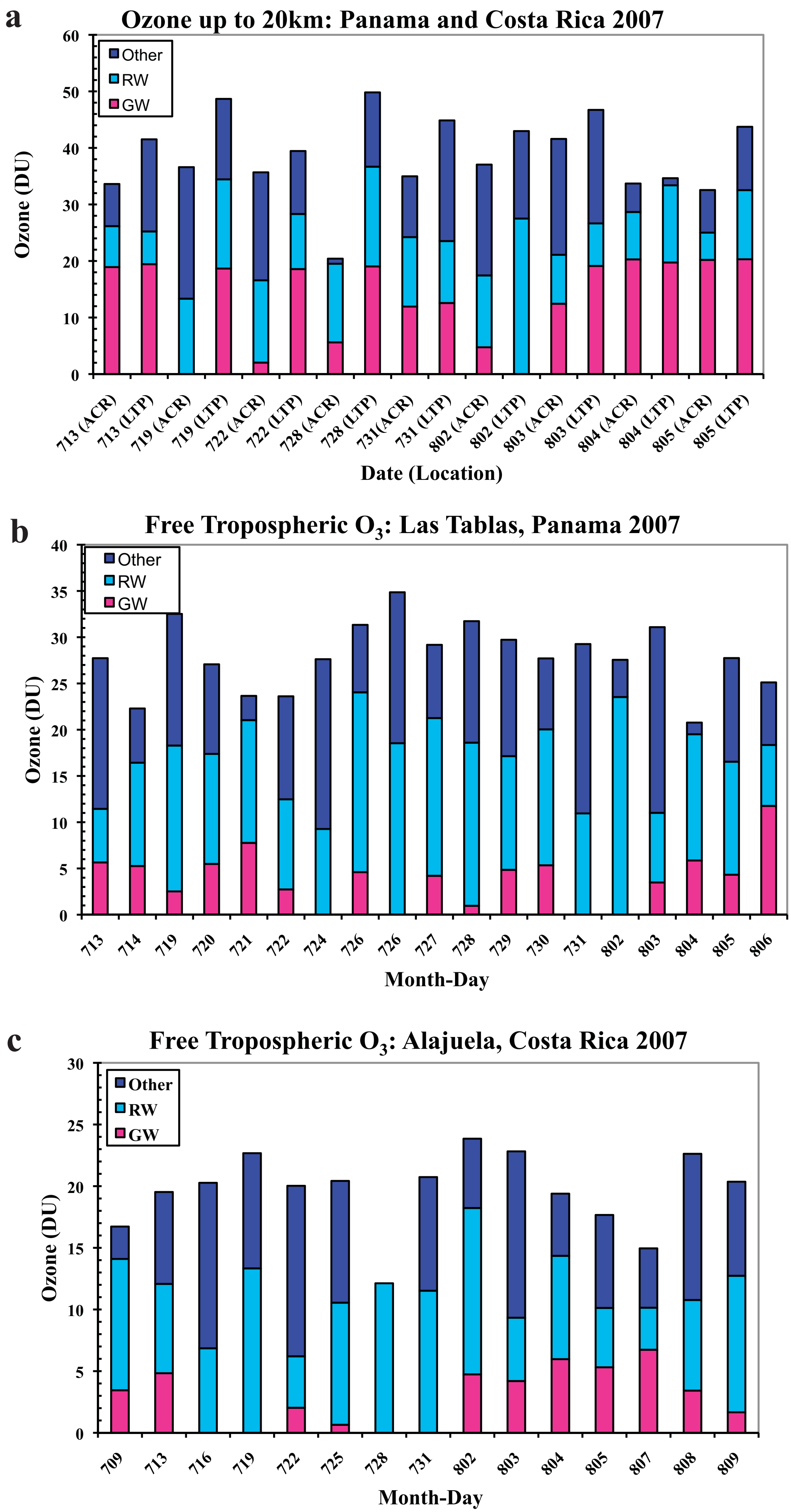
a
Ozone up to 20km: Panama and Costa Rica 2007
Other
RW
GW
Ozone (DU)
0
10
20
30
40
50
60
713 (ACR)
713 (LTP)
719 (ACR)
719 (LTP)
722 (ACR)
722 (LTP)
728 (ACR)
728 (LTP)
731(ACR)
731 (LTP)
802 (ACR)
802 (LTP)
803 (ACR)
803 (LTP)
804 (ACR)
804 (LTP)
805 (ACR)
805 (LTP)
Date (Location)
b
Free Tropospheric O_3: Las Tablas, Panama 2007
Other
RW
GW
Ozone (DU)
0
5
10
15
20
25
30
35
40
713
714
719
720
721
722
724
726
726
727
728
729
730
731
802
803
804
805
806
Month-Day
c
Free Tropospheric O_3: Alajuela, Costa Rica 2007
Other
RW
GW
Ozone (DU)
0
5
10
15
20
25
30
709
713
716
719
722
725
728
731
802
803
804
805
807
808
809
Month-Day

FIGURE 5

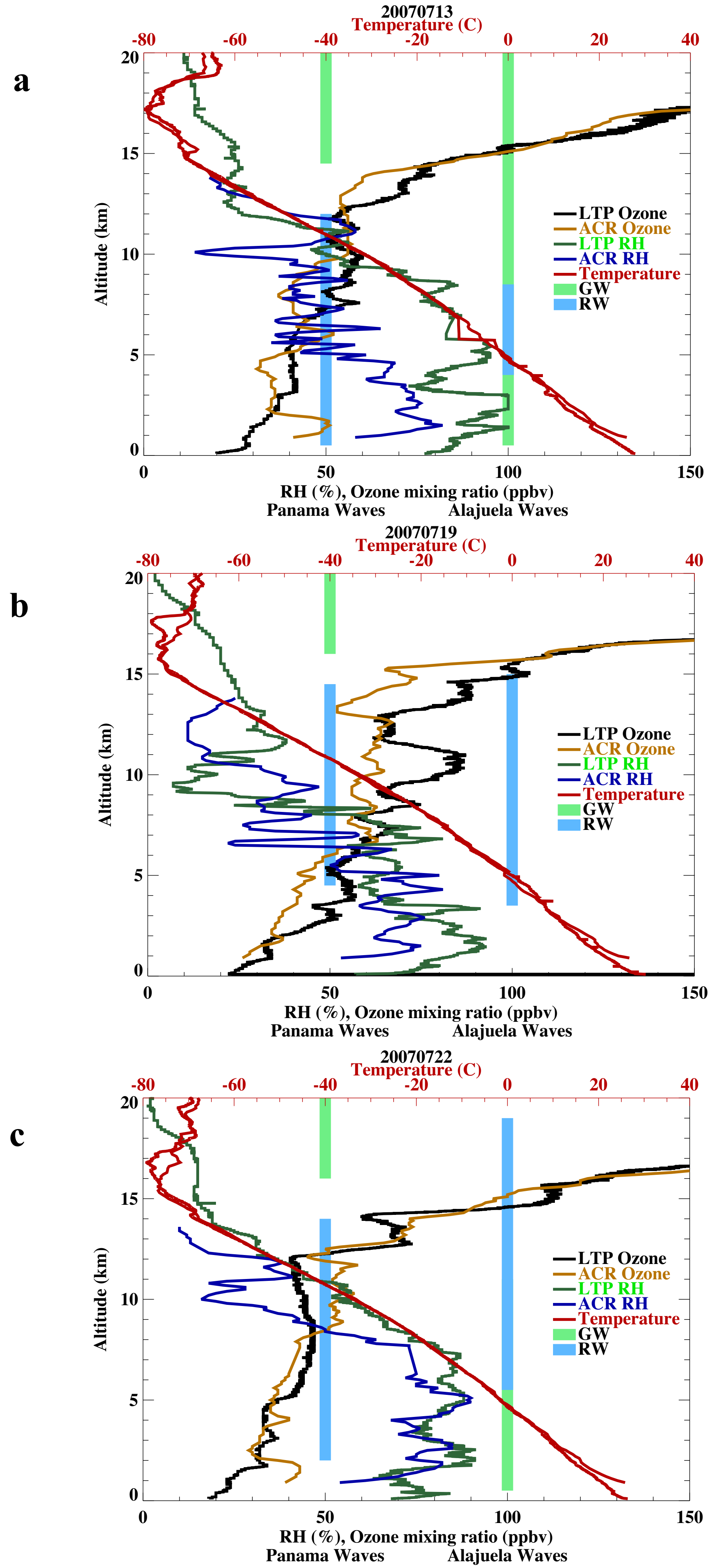
a
20070713
Temperature (C)
-80
-60
-40
-20
0
20
40
Altitude (km)
LTP Ozone
ACR Ozone
LTP RH
ACR RH
Temperature
GW
RW
RH (%), Ozone mixing ratio (ppbv)
Panama Waves
Alajuela Waves
b
20070719
c
20070722

FIGURE 6

a

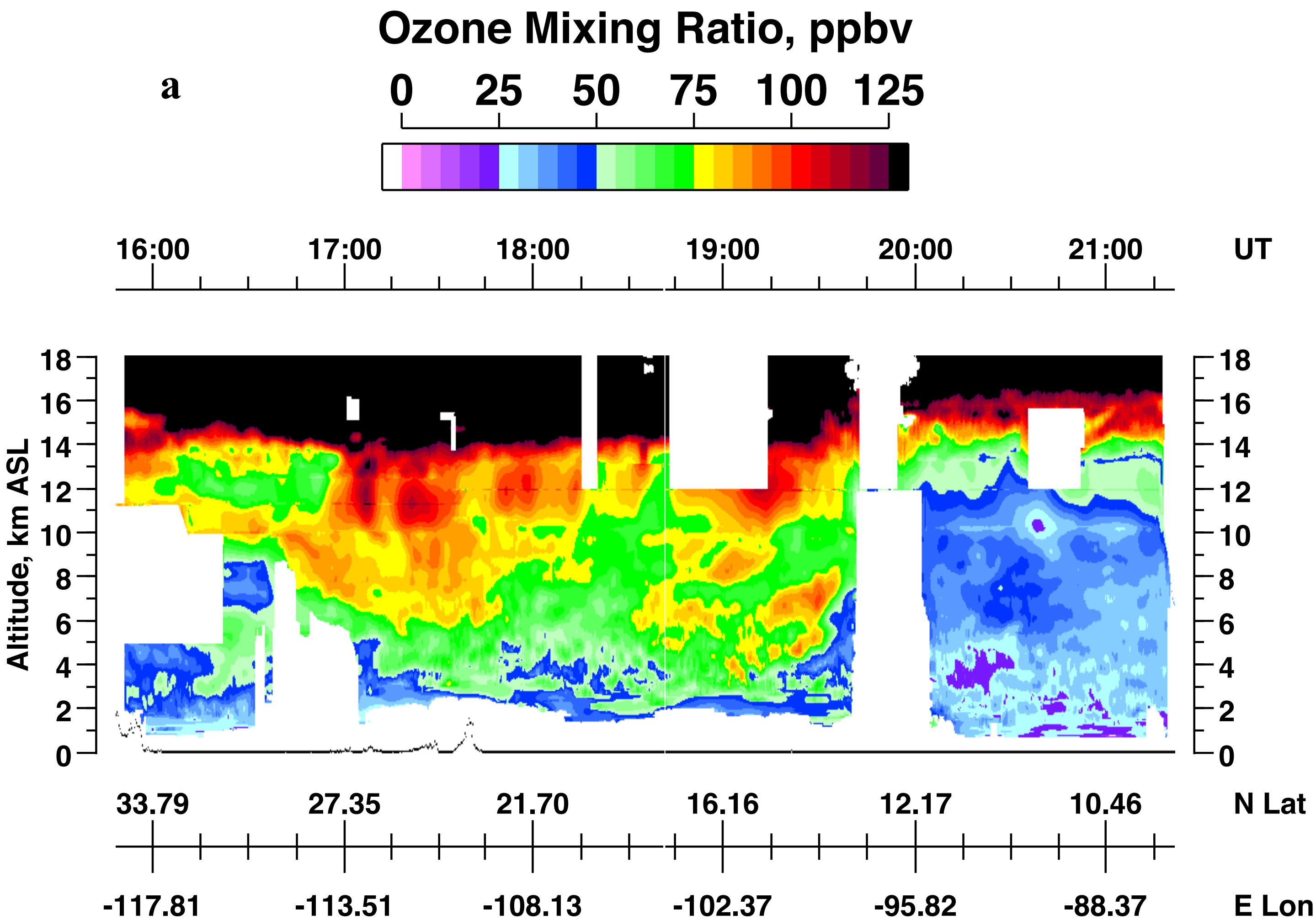
Ozone Mixing Ratio, ppbv
0 25 50 75 100 125
16:00 17:00 18:00 19:00 20:00 21:00 UT
Altitude, km ASL
18 16 14 12 10 8 6 4 2 0
33.79 27.35 21.70 16.16 12.17 10.46 N Lat
-117.81 -113.51 -108.13 -102.37 -95.82 -88.37 E Lon

b

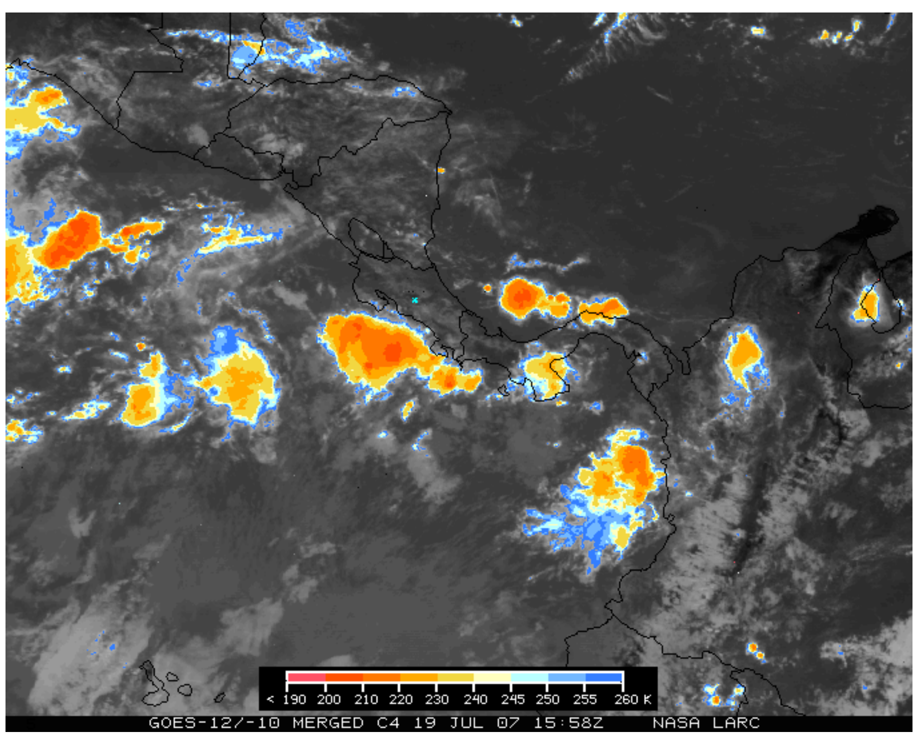
< 190 200 210 220 230 240 245 250 255 260 K
GOES-12/-10 MERGED C4 19 JUL 07 15:58Z NASA LARC

FIGURE 7

c

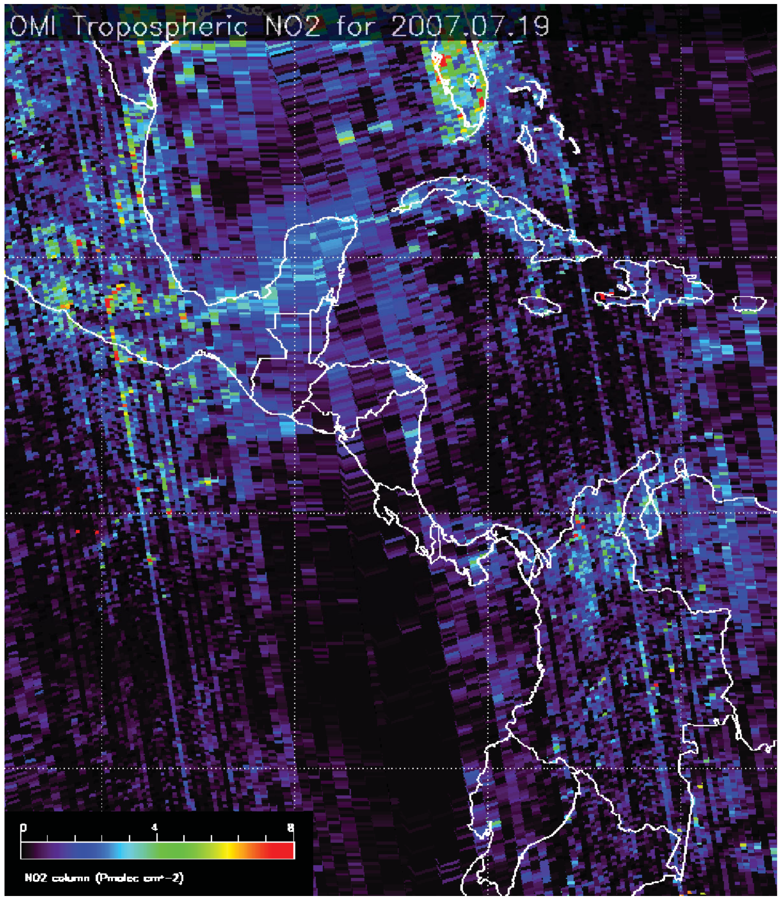

d

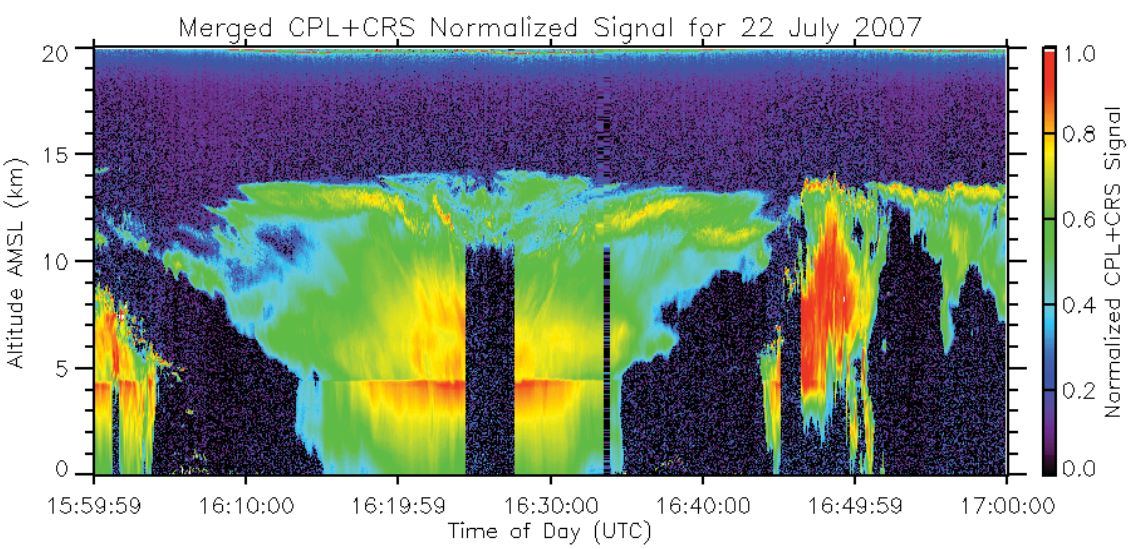

FIGURE 7 (continued)

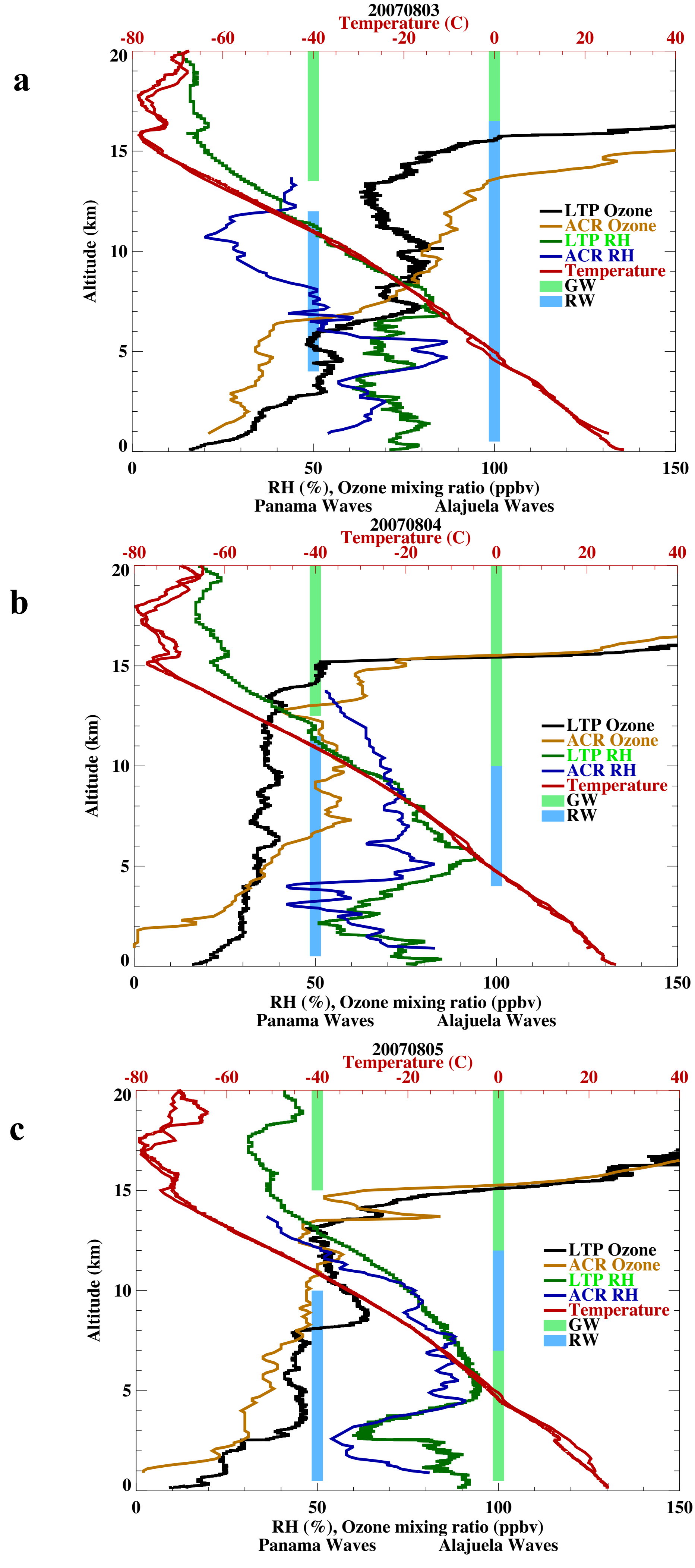
a
20070803
Temperature (C)
-80
-60
-40
-20
0
20
40
Altitude (km)
0
5
10
15
20
LTP Ozone
ACR Ozone
LTP RH
ACR RH
Temperature
GW
RW
0
50
100
150
RH (%), Ozone mixing ratio (ppbv)
Panama Waves
Alajuela Waves
b
20070804
Temperature (C)
Altitude (km)
LTP Ozone
ACR Ozone
LTP RH
ACR RH
Temperature
GW
RW
RH (%), Ozone mixing ratio (ppbv)
Panama Waves
Alajuela Waves
c
20070805
Temperature (C)
Altitude (km)
LTP Ozone
ACR Ozone
LTP RH
ACR RH
Temperature
GW
RW
RH (%), Ozone mixing ratio (ppbv)
Panama Waves
Alajuela Waves

FIGURE 8

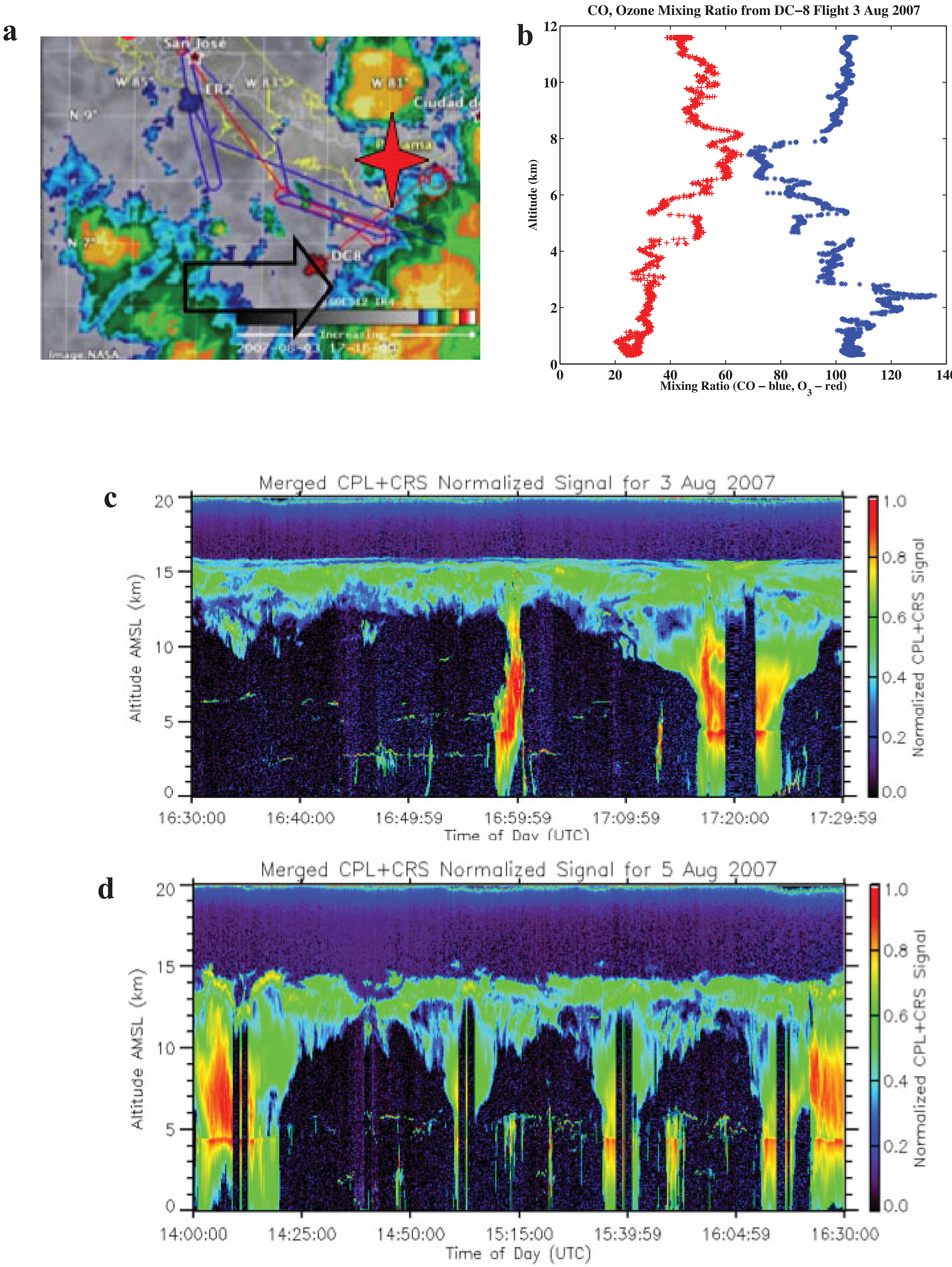
a
San José
ER2
DC8
Image NASA
b
CO, Ozone Mixing Ratio from DC−8 Flight 3 Aug 2007
Altitude (km)
Mixing Ratio (CO − blue, O3 − red)
0 20 40 60 80 100 120 140
0 2 4 6 8 10 12
c
Merged CPL+CRS Normalized Signal for 3 Aug 2007
Altitude AMSL (km)
Time of Day (UTC)
16:30:00 16:40:00 16:49:59 16:59:59 17:09:59 17:20:00 17:29:59
Normalized CPL+CRS Signal
0.0 0.2 0.4 0.6 0.8 1.0
d
Merged CPL+CRS Normalized Signal for 5 Aug 2007
Altitude AMSL (km)
Time of Day (UTC)
14:00:00 14:25:00 14:50:00 15:15:00 15:39:59 16:04:59 16:30:00
Normalized CPL+CRS Signal
0.0 0.2 0.4 0.6 0.8 1.0

FIGURE 9

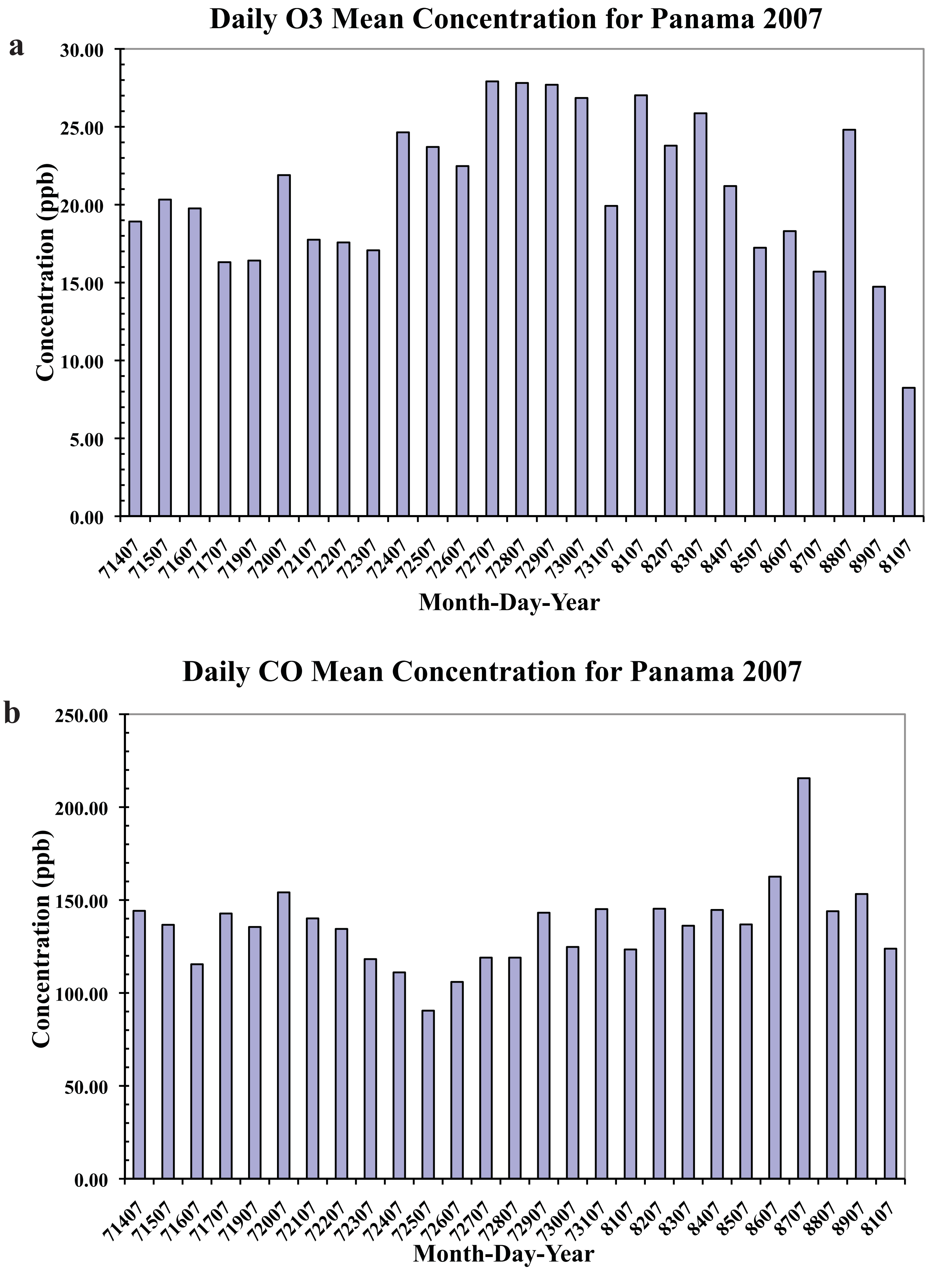

Daily O3 Mean Concentration for Panama 2007
a
30.00
25.00
20.00
15.00
10.00
5.00
0.00
Concentration (ppb)
71407
71507
71607
71707
71907
72007
72107
72207
72307
72407
72507
72607
72707
72807
72907
73007
73107
8107
8207
8307
8407
8507
8607
8707
8807
8907
8107
Month-Day-Year
Daily CO Mean Concentration for Panama 2007
b
250.00
200.00
150.00
100.00
50.00
0.00
Concentration (ppb)
71407
71507
71607
71707
71907
72007
72107
72207
72307
72407
72507
72607
72707
72807
72907
73007
73107
8107
8207
8307
8407
8507
8607
8707
8807
8907
8107
Month-Day-Year

FIGURE 10

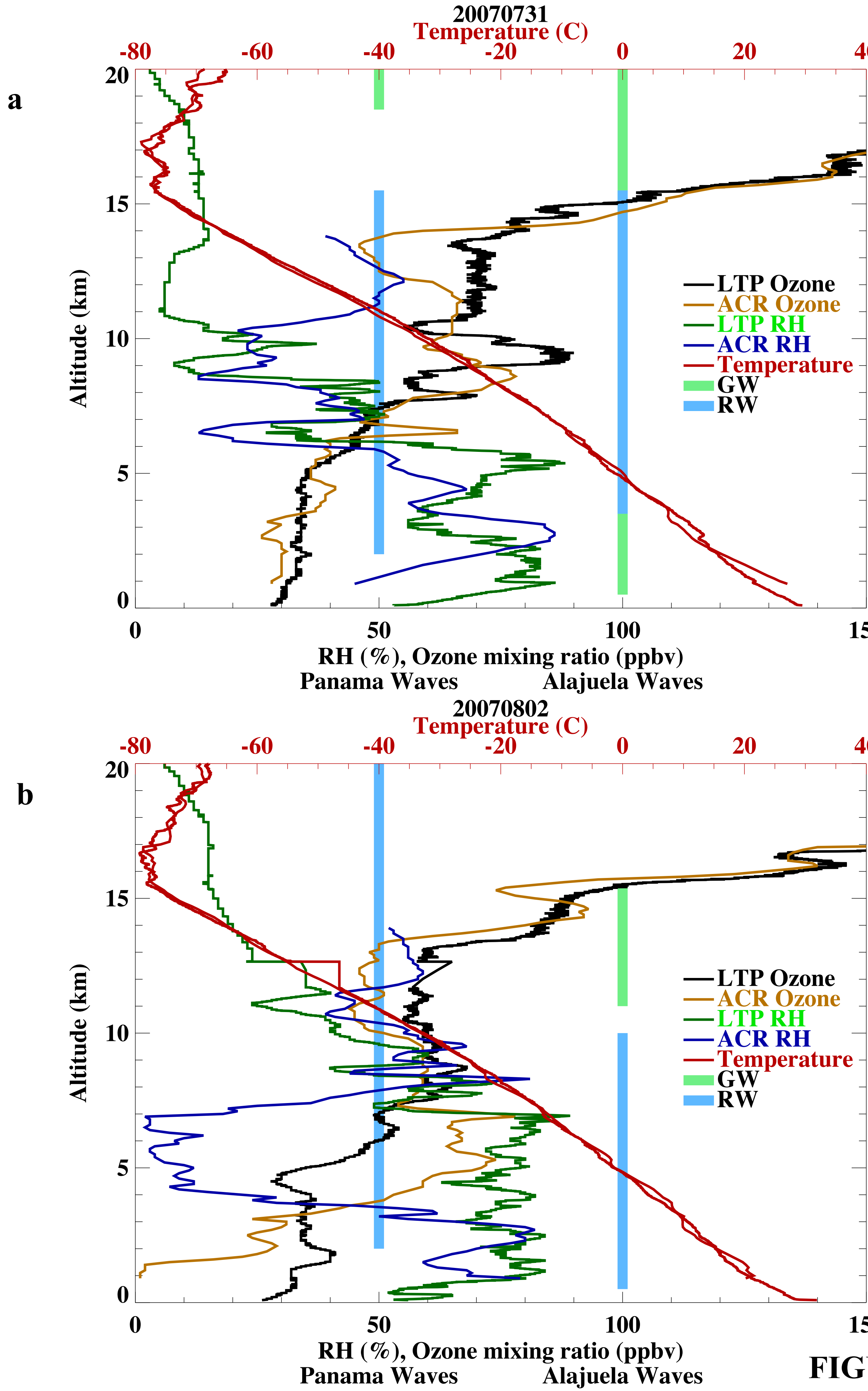

a
20070731
Temperature (C)
-80
-60
-40
-20
0
20
40
20
15
10
5
0
Altitude (km)
LTP Ozone
ACR Ozone
LTP RH
ACR RH
Temperature
GW
RW
0
50
100
150
RH (%), Ozone mixing ratio (ppbv)
Panama Waves
Alajuela Waves
b
20070802
Temperature (C)
-80
-60
-40
-20
0
20
40
20
15
10
5
0
Altitude (km)
LTP Ozone
ACR Ozone
LTP RH
ACR RH
Temperature
GW
RW
0
50
100
150
RH (%), Ozone mixing ratio (ppbv)
Panama Waves
Alajuela Waves

FIGURE 11

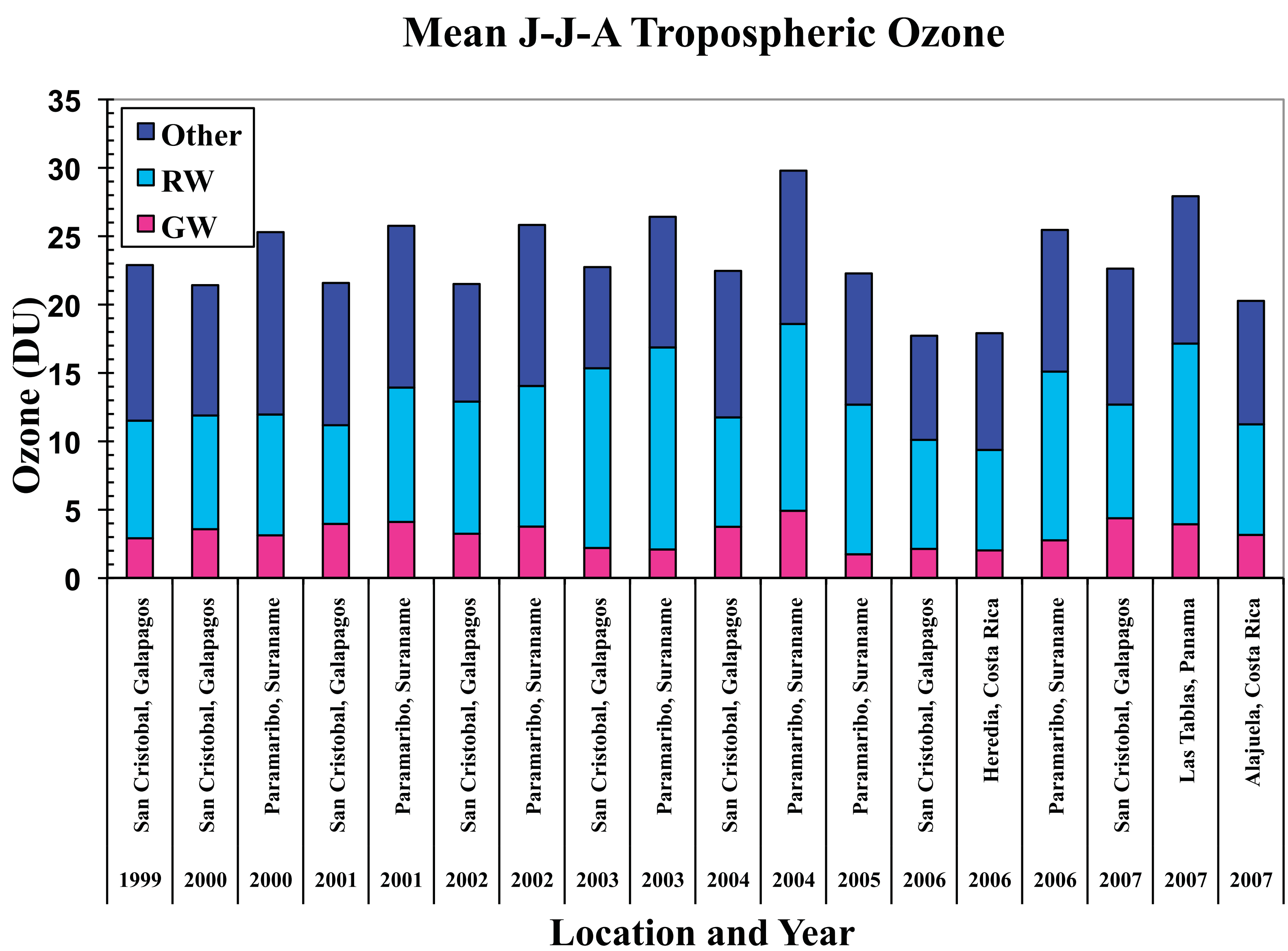
Mean J-J-A Tropospheric Ozone
Ozone (DU)
0
5
10
15
20
25
30
35
Other
RW
GW
San Cristobal, Galapagos 1999
San Cristobal, Galapagos 2000
Paramaribo, Suraname 2000
San Cristobal, Galapagos 2001
Paramaribo, Suraname 2001
San Cristobal, Galapagos 2002
Paramaribo, Suraname 2002
San Cristobal, Galapagos 2003
Paramaribo, Suraname 2003
San Cristobal, Galapagos 2004
Paramaribo, Suraname 2004
Paramaribo, Suraname 2005
San Cristobal, Galapagos 2006
Heredia, Costa Rica 2006
Paramaribo, Suraname 2006
San Cristobal, Galapagos 2007
Las Tablas, Panama 2007
Alajuela, Costa Rica 2007
Location and Year

FIGURE 12

a

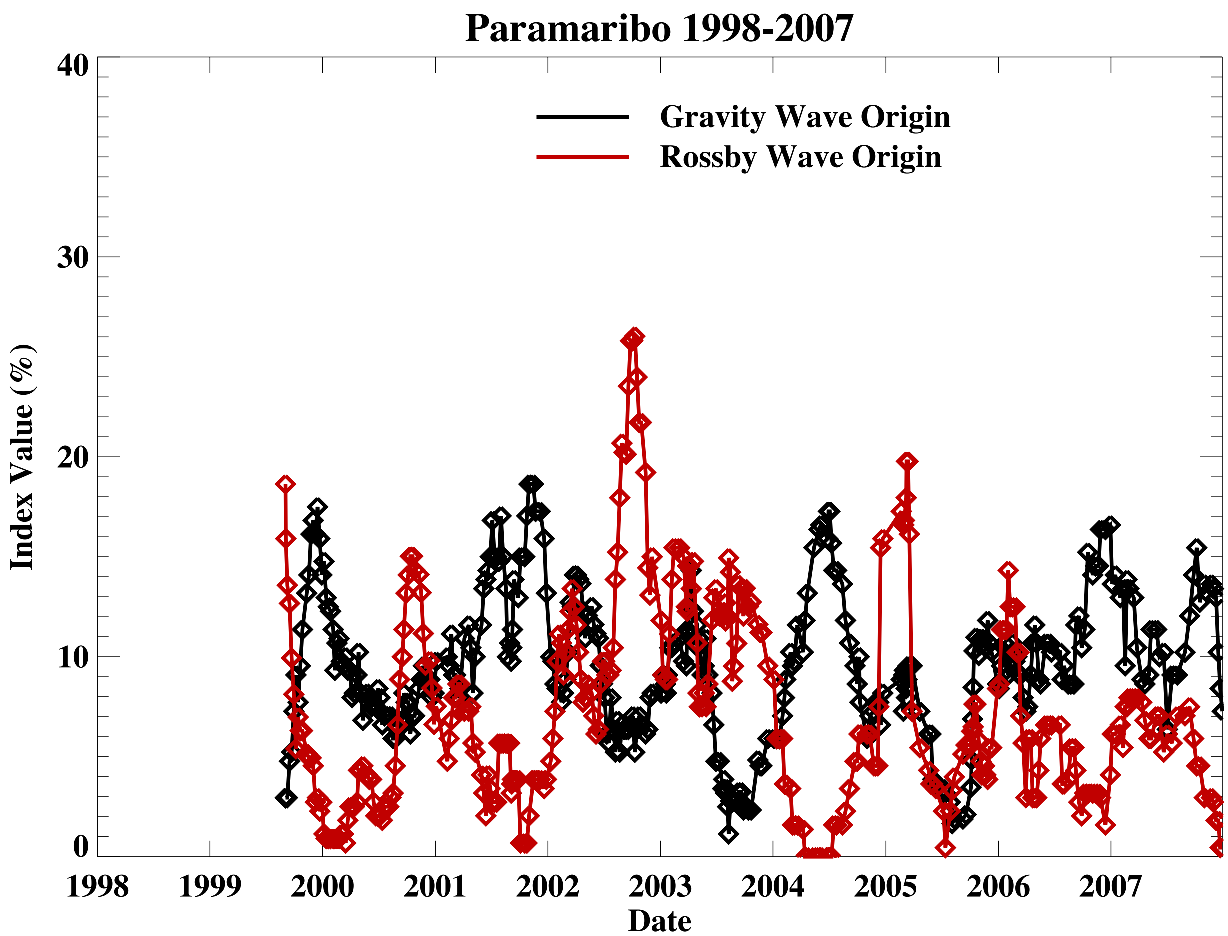

Paramaribo 1998-2007
Gravity Wave Origin
Rossby Wave Origin
Index Value (%)
0
10
20
30
40
1998
1999
2000
2001
2002
2003
2004
2005
2006
2007
Date

b

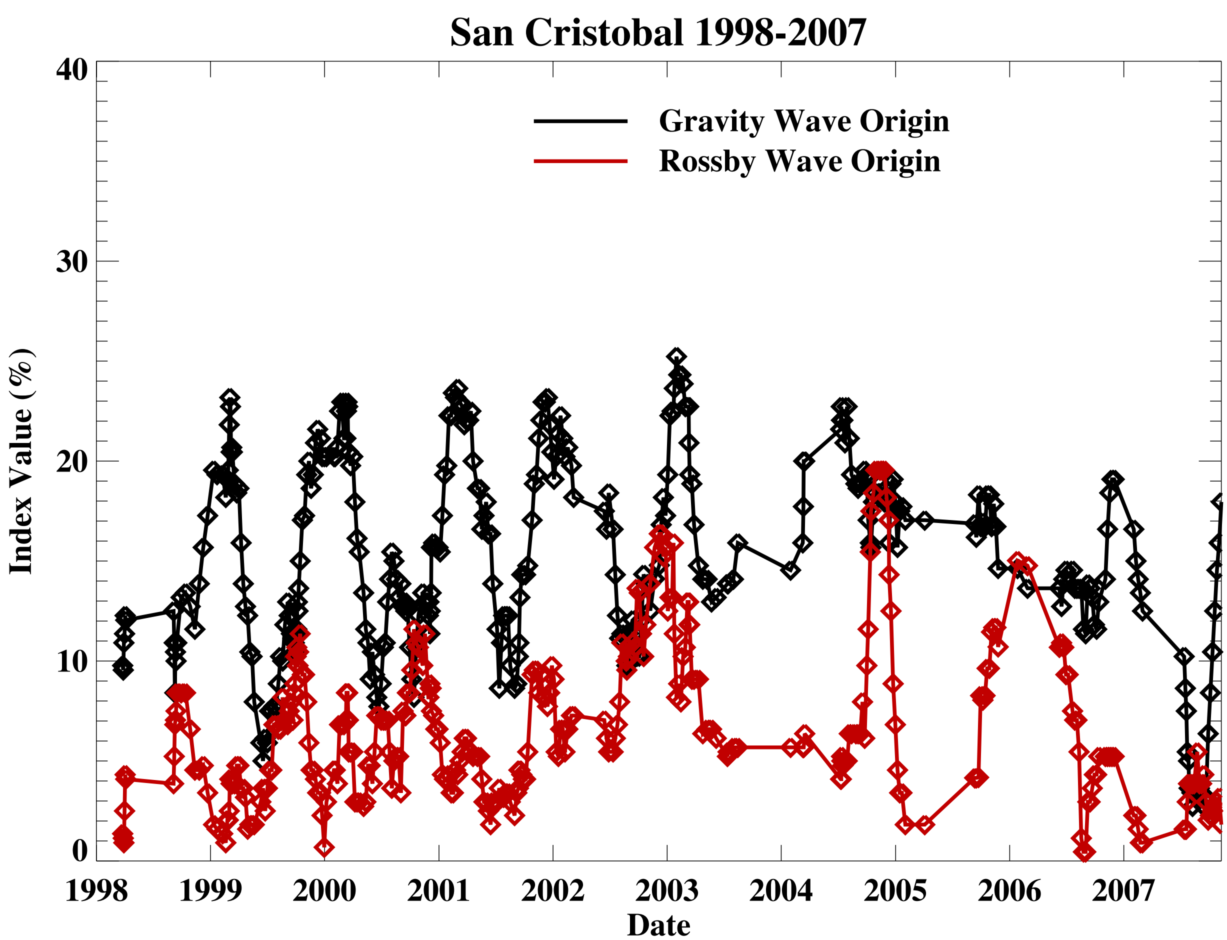

San Cristobal 1998-2007
Gravity Wave Origin
Rossby Wave Origin
Index Value (%)
0
10
20
30
40
1998
1999
2000
2001
2002
2003
2004
2005
2006
2007
Date

FIGURE 13